Open Archive Toulouse Archive Ouverte (OATAO)

OATAO is an open access repository that collects the work of Toulouse researchers and makes it freely available over the web where possible.

Any correspondence concerning this service should be sent to the repository administrator: staff-oatao@inp-toulouse.fr

Thermodynamic modelling of the Cr–Fe–Ni–O system

Lina Kjellqvist [a,*], Malin Selleby [a], Bo Sundman [b]

[a] *Materials Science and Engineering, Royal Institute of Technology, 10044 Stockholm, Sweden*
[b] *CIRIMAT, ENSIACET, 118 route de Narbonne, 31077 Toulouse, France*

ABSTRACT

There is a need to describe the influence of oxygen on high alloyed steels, both regarding oxidation processes – as in the formation of oxide layers – and regarding steel/slag processes in a metallurgical context. As a first step and in order to be able to perform calculations and simulations on these different processes, the thermodynamic properties need to be described, as done for the Cr–Fe–Ni–O system. Previous attempts to describe this system has resulted in an inconsistent description, more specifically concerning the spinel phase. The aim of the present study is to obtain a consistent thermodynamic database for the Cr–Fe–Ni–O system with an emphasis on the modelling of the spinel phase. The solid phases are described using the compound energy formalism and the metallic and ionized liquid is modelled using the ionic two-sublattice model. A complete list of all binary and higher order parameters is included.

1. Introduction

The Cr–Fe–Ni–O system is of fundamental importance when describing the influence of oxygen on stainless steels. The solid part is of interest for a number of processes: formation of oxide layers on stainless steels, internal oxidation, sintering processes and high temperature corrosion. The liquid phases (metal and slag) are of interest for metallurgical applications, e.g. the interaction between high alloyed steel and its slag.

Recently, the Cr–Fe–Ni–O system has been analysed by [1], who used the associate solution model [2] to describe the liquid phase. The ionic two-sublattice model was used by [3–5], respectively for the assessments of the Cr–Fe–O, Cr–Ni–O and Fe–Ni–O systems. The metallic ternary, Fe–Cr–Ni, was described by [6,7]. In the present work both the metallic and the oxide liquid are modelled using the ionic two-sublattice model [8,9]. The substitutional liquid model used in the metallic system can readily be translated to the ionic two-sublattice model. The solid phases are all described using the compound energy formalism (CEF) [10].

The aim of this study was to obtain a consistent thermodynamic database for the Cr–Fe–Ni–O system. Most of the previously assessed sub-systems have been accepted, but some parts have been reassessed. Descriptions of the spinel phase for the Fe_3O_4, $FeCr_2O_4$, $NiFe_2O_4$ and $NiCr_2O_4$ simple spinels were incompatible using the original descriptions, but are now consistent. The description of the liquid phase in the Cr–Fe–O and Cr–Ni–O

systems had to be reassessed due to unwanted miscibility gaps found in the previous assessments. An extensive review of the experimental data on the C–Cr–Fe–Ni–O system was given by [1]. Those references are not repeated in this paper.

We are currently working on developing a database for a larger oxide system, where the Cr–Fe–Ni–O is the core system. In the near future, C and Mn will also be included in this database, and later on extended with more elements. The liquid model is compatible with the model used in a parallel work on the Al_2O_3–CaO–Fe–O–MgO–SiO_2 system [11,12].

2. Thermodynamic models

The CEF was developed to describe phases using two or more sublattices and is widely used in CALPHAD assessments [13,14]. The concept constituent array is introduced, which specifies one or more constituent on each sublattice and is denoted by I. The constituent arrays can be of different orders and the zeroth order has one constituent on each sublattice. The Gibbs energy for a phase is described as:

$$G_m = \sum_{I_0} P_{I_0}(Y) \, {}^{o}G_{I_0} + RT \sum_{s=1}^{n} a_s \sum_{i=1}^{n_s} y_i^s \ln(y_i^s) + {}^{\text{phys}}G_m + {}^{E}G_m \qquad (1)$$

where I_0 is a constituent array of zeroth order and $P_{I_0}(Y)$ is the corresponding product of the site fractions specified by I_0. ${}^{o}G_{I_0}$ represents the Gibbs energy of the compound I_0. The factor a_s is the number of sites on sublattice s and y_i^s denotes the site-fraction of component i on sublattice s. ${}^{\text{phys}}G_m$ represent the contribution to the Gibbs energy due to physical properties like the magnetic

* Corresponding author. Tel.: +46 8 7908313; fax: +46 8 100411.
E-mail address: lina@mse.kth.se (L. Kjellqvist).

transitions and $^{E}G_m$ is the excess Gibbs energy:

$$^{E}G_m = \sum_{I_1} P_{I_1}(Y)L_{I_1} + \sum_{I_2} P_{I_2}(Y)L_{I_2} + \cdots \tag{2}$$

where I_1 is a constituent array of first order and L_{I_1} is the interaction parameters defined by I_1. A constituent array of first order has two constituents in one sublattice but only one in the remaining sublattices. A constituent array of second order could have either three interacting constituents on one sublattice or two interacting constituents on two different sublattices. The second case is a so-called reciprocal parameter. Higher order terms may also be added.

2.1. Magnetic properties

The solid metallic phases and some of the solid oxide phases undergo a magnetic transition characterised by a λ-peak in the heat capacity curve. The magnetic contribution to the Gibbs energy is given by the model proposed by [15] and adapted by [16].

The magnetic contribution to the Gibbs energy is described by:

$$^{\text{magn}}G = RT\ln(\beta + 1)f(\tau) \tag{3}$$

where $\tau = T/T_C$ and β is the Bohr magneton number. β and T_C are model parameters that may be determined through an optimisation procedure.

For $\tau < 1$:

$$f(\tau) = 1 - \left[\frac{79\tau^{-1}}{140p} + \frac{474}{497}\left(\frac{1}{p} - 1\right)\left(\frac{\tau^3}{6} + \frac{\tau^9}{135} + \frac{\tau^{15}}{600}\right)\right]\bigg/A. \tag{4}$$

For $\tau > 1$:

$$f(\tau) = -\left(\frac{\tau^{-5}}{10} + \frac{\tau^{-15}}{315} + \frac{\tau^{-25}}{1500}\right)\bigg/A \tag{5}$$

where $A = \frac{518}{1125} + \frac{11692}{15975}\left(\frac{1}{p} - 1\right)$ and p is a number that depends on the structure.

2.2. Liquid

Within the framework of the CEF, the ionic two-sublattice liquid model was developed [8,9]. The same model can be used both for metallic and oxide melts. At low levels of oxygen, the model becomes equivalent to a substitutional solution model between metallic atoms. Two sublattices are assumed, one containing charged cations and one containing charged anions, neutrals and vacancies:

$$(C_i^{v_i})_P(A_j^{v_j}, \text{Va}^{-Q}, B_k^0)_Q$$

where C represents cations, A anions, Va vacancies and B neutrals. The indices i, j and k denotes specific constituents. Charged vacancies are introduced on the second sublattice to keep electroneutrality when the composition approaches metallic liquid. The site numbers, P and Q, on the sublattices vary so that electroneutrality is maintained:

$$P = \sum_j y_{A_j}(-v_j) + Qy_{\text{Va}} \tag{6}$$

$$Q = \sum_i y_{C_i} v_i. \tag{7}$$

The Gibbs energy of the liquid phase is expressed by:

$$G_m = \sum_i \sum_j y_{C_i} y_{A_j} {}^oG_{C_i:A_j} + Qy_{\text{Va}} \sum_i y_{C_i} {}^oG_{C_i} + Q\sum_k y_{B_k} {}^oG_{B_k}$$
$$+ RTP \sum_i y_{C_i}\ln(y_{C_i}) + RTQ \sum_j y_{A_j}\ln(y_{A_j}) + RTQy_{\text{Va}}\ln(y_{\text{Va}})$$
$$+ RTQ \sum_k y_{B_k}\ln(y_{B_k}) + {}^{E}G_m. \tag{8}$$

The excess Gibbs energy expression is given by

$$^{E}G_m = \sum_{i_1}\sum_{i_2}\sum_j y_{C_{i_1}} y_{C_{i_2}} y_{A_j} L_{C_{i_1},C_{i_2}:A_j} + Qy_{\text{Va}}^2 \sum_{i_1}\sum_{i_2} y_{C_{i_1}} y_{C_{i_2}} L_{C_{i_1},C_{i_2}:\text{Va}}$$
$$+ y_{\text{Va}}\sum_i\sum_j y_{C_i} y_{A_j} L_{C_i:A_j,\text{Va}} + \sum_i\sum_j\sum_k y_{C_i} y_{A_j} y_{B_k} L_{C_i:A_j,B_k}$$
$$+ Qy_{\text{Va}}\sum_i\sum_k y_{C_i} y_{B_k} L_{C_i:B_k,\text{Va}}$$
$$+ Qy_{\text{Va}}^3 \sum_{i_1}\sum_{i_2}\sum_{i_3} y_{C_{i_1}} y_{C_{i_2}} y_{C_{i_3}} L_{C_{i_1},C_{i_2},C_{i_3}:\text{Va}}$$
$$+ y_{\text{Va}}\sum_{i_1}\sum_{i_2}\sum_j y_{C_{i_1}} y_{C_{i_2}} y_{A_j} L_{C_{i_1},C_{i_2}:A_j,\text{Va}}. \tag{9}$$

A colon is used to separate species on different sublattices and a comma is used to separate species on the same sublattice. Eq. (9) is not a complete list of interaction parameters, only those actually used in the present system. The first five terms are binary interactions and the last two are ternary interactions.

In the Cr–Fe–Ni–O system, considering Cr^{+3}, Fe^{+2}, Ni^{+2}, O^{-2}, $FeO_{1.5}$ and vacancies, the liquid phase is described as:

$$(Cr^{+3}, Fe^{+2}, Ni^{+2})_P(O^{-2}, \text{Va}^{-Q}, FeO_{1.5})_Q.$$

The liquid phase in the Fe–O system was first modelled with $(Fe^{+2}, Fe^{+3})_P$ $(O^{-2}, \text{Va}^{-Q})_Q$ [17], but later Fe^{+3} was replaced by a neutral species, $FeO_{1.5}$ [18]. This change was imposed by an equivalent change for Al-containing system where Al^{+3} was replaced by $AlO_{1.5}$ in order to better control the unwanted reciprocal miscibility gaps that occurred in e.g. Al_2O_3–CaO–SiO_2. However, even though a new model for liquid Al_2O_3 (without $AlO_{1.5}$) has been developed [19], the $FeO_{1.5}$ species has been kept.

2.3. Halite

The wustite (FeO) and bunsenite (NiO) phases are isomorphous both having the NaCl-type structure (Strukturbericht B1), with generic name halite. The halite phase is described using a model within the CEF with two sublattices; one for metal ions and one for oxygen. Wustite has a considerable solid solubility, due to the fact that iron has two valency states, Fe^{+2} and Fe^{+3}. Wustite is stable up to an oxygen content of $x_O = 0.55$ at approximately 1425 °C. In order to model deviation from stoichiometry and maintain the electroneutrality, vacancies must be introduced to the cation sublattice. The same model is used to model the non-stoichiometry of bunsenite. The solubility of Cr in wustite and bunsenite is modelled with Cr^{+3} on the cation lattice. The phase is thus represented as:

$$(Cr^{+3}, Fe^{+2}, Fe^{+3}, Ni^{+2}, Ni^{+3}, Va)_1(O^{-2})_1.$$

Bunsenite undergoes a magnetic transition at 519 K. The magnetic contribution to the Gibbs energy is described using Eq. (3). The $Ni^{+2}:O^{-2}$ and $Ni^{+3}:O^{-2}$ compounds have been given the same magnetic properties, while the others are set to zero. In the previous assessment of the Cr–Ni–O system [3], also the $Cr^{+3}:O^{-2}$ and $\text{Va}:O^{-2}$ compounds had been given the same magnetic properties. As the $\text{Va}:O^{-2}$ compound is included in other phases described using the same model, e.g. wustite, a more realistic model would be that the magnetic properties of that compound are set to zero. Further, if the $Cr^{+3}:O^{-2}$ compound is given non-zero values for the magnetic properties, wustite with some Cr solubility would, according to that description, be magnetic, despite wustites non-magnetic behaviour. This is considered unrealistic, why T_C and β for the $Cr^{+3}:O^{-2}$ and $\text{Va}:O^{-2}$ compounds in this study are given the values zero.

2.4. Corundum

Hematite (Fe_2O_3) and eskolaite (Cr_2O_3) are isomorphous (Strukturbericht $D5_1$), and described with a model within the CEF using three sublattices. The generic phase name is corundum. The hematite composition is very close to stoichiometric Fe_2O_3 and it was treated as a stoichiometric compound in previous assessments [17,4,5]. To be able to use this description for modelling diffusivity of ionic species, hematite is here modelled with an additional interstitial sublattice with Fe^{+3} and vacancies. To maintain electroneutrality, divalent Fe is introduced in the first sublattice:

$$(Fe^{+2}, Fe^{+3})_2(Fe^{+3}, Va)_1(O^{-2})_3.$$
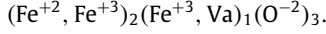
The compound $^oG_{Fe^{+3}:Va:O^{-2}}$ adopts the value for pure Fe_2O_3 from [17]. This is the only compound which is electrically neutral, the others will be present only in neutral combinations. There is a neutral line between $^oG_{Fe^{+3}:Va:O^{-2}}$ and $\frac{2}{3}\,^oG_{Fe^{+2}:Fe^{+3}:O^{-2}} + \frac{1}{3}$ $^oG_{Fe^{+2}:Va:O^{-2}}$. There is only experimental information to optimise two parameters; the stoichiometric compound (Fe_2O_3) and where, along the neutral line, the solution resides. The other two parameters are given arbitrary values. The electric charge of the phase, $^oG_{Fe^{+2}:Va:O^{-2}} = \,^oG_{Fe^{+3}:Va:O^{-2}}$ was chosen as reference. The energy of the reciprocal reaction,

$$\Delta G_{23:3V} = \,^oG_{Fe^{+2}:Va:O^{-2}} + \,^oG_{Fe^{+3}:Fe^{+3}:O^{-2}}$$
$$- \,^oG_{Fe^{+2}:Fe^{+3}:O^{-2}} - \,^oG_{Fe^{+3}:Va:O^{-2}} \quad (10)$$

is assumed to be zero. The equation to be able to optimise the deviation from stoichiometry reads:

$$\frac{2}{3}\,^oG_{Fe^{+2}:Fe^{+3}:O^{-2}} + \frac{1}{3}\,^oG_{Fe^{+2}:Va:O^{-2}} = \,^oG_{Fe^{+3}:Va:O^{-2}} + A' + B'T. \quad (11)$$

The following relations are obtained:

$$^oG_{Fe^{+3}:Va:O^{-2}} = G^{hematite}$$
$$^oG_{Fe^{+2}:Va:O^{-2}} = \,^oG_{Fe^{+3}:Va:O^{-2}}$$
$$^oG_{Fe^{+2}:Fe^{+3}:O^{-2}} = \,^oG_{Fe^{+3}:Va:O^{-2}} + A + BT$$
$$^oG_{Fe^{+3}:Fe^{+3}:O^{-2}} = \,^oG_{Fe^{+3}:Va:O^{-2}} + A + BT \quad (12)$$

where $A = \frac{3}{2}A'$ and $B = \frac{3}{2}B'$.

The solubility of Ni in eskolaite was modelled by [3] by adding Ni^{+2} ions on the interstitial sublattice. The whole composition range of the phase is thus represented by:

$$(Cr^{+2}, Cr^{+3}, Fe^{+2}, Fe^{+3})_2(Cr^{+3}, Fe^{+3}, Ni^{+2}, Va)_1(O^{-2})_3.$$
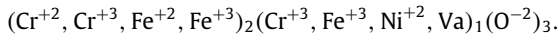
The end-members $Fe^{+2}:Ni^{+2}:O^{-2}$ and $Fe^{+3}:Ni^{+2}:O^{-2}$ were given arbitrary high values to give a minimal solubility of Ni in Fe_2O_3, since no solubility has been reported in the literature.

Hematite and eskolaite undergo magnetic transitions at 943 and 306 K, respectively. All compounds with Cr ions on the first sublattice has been given the same magnetic properties, originally from [3]. All compounds with Fe ions on the first sublattice has also been given the same magnetic properties, originally from [17]. It makes very small difference what values are chosen for the magnetic properties for the $Fe^{+2}:Ni^{+2}:O^{-2}$ and $Fe^{+3}:Ni^{+2}:O^{-2}$ compounds, since the solubility of Ni in Fe_2O_3 is so low. Fe_2O_3 and Cr_2O_3 are completely miscible and the magnetic properties of the mixture are assumed to vary linearly, i.e. $T_C(Fe^{+3}, Cr^{+3}:Va:O^{-2}) = 0$ and $\beta(Fe^{+3}, Cr^{+3}:Va:O^{-2}) = 0$.

2.5. Spinel

The spinel phase (Strukturbericht $H1_1$) properties are based on those of the five simple spinels; Fe_3O_4, $FeCr_2O_4$, Cr_3O_4, $NiFe_2O_4$, and $NiCr_2O_4$. The spinel structure has oxygen ions in an fcc sublattice, with divalent and trivalent metallic ions in the octahedral and tetrahedral interstitial sublattices. Four sublattices are used to model the spinel phase, where the first sublattice represents tetrahedral sites and the second and third sublattices represent octahedral sites. A normal spinel has the trivalent ions on the octahedral sites and the divalent ions on the tetrahedral sites. If the tetrahedral sites are occupied by trivalent ions the spinel is referred to as inverse. The third interstitial sublattice is needed to describe a deviation from stoichiometry toward excess metal, accomplished by the introduction of Fe^{+2} as interstitials on octahedral sites that are normally empty. The presence of Cr^{+2} on an interstitial sublattice was however not considered earlier. After the assessments of the Cr–Fe–O [4] and Cr–Ni–O [3] systems were published, [20] have experimentally determined cation tracer diffusion coefficients. They observed an oxygen activity dependence indicating that the diffusion of Cr and Fe in $(Cr_xFe_{1-x})_{3-\delta}O_4$ at high oxygen activities is governed by cation vacancies and at low oxygen activities by cation interstitials. To be able to reproduce that behaviour the introduction of Cr^{+2} on the interstitial sublattice is necessary. The spinel phase is thus modelled as:

$$(Cr^{+2}, Cr^{+3}, Fe^{+2}, Fe^{+3}, Ni^{+2})_1(Cr^{+3}, Fe^{+2}, Fe^{+3}, Ni^{+2}, Va)_2$$
$$(Cr^{+2}, Fe^{+2}, Va)_2(O^{-2})_4.$$
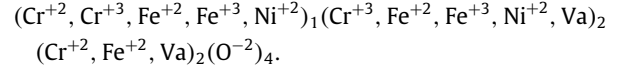
75 combinations are possible and most of these end-members have a net charge and can be present only in neutral combinations, but each end-member must be given a Gibbs energy value. In practice the number of independent parameters is much less than this. [17], for example, used only four independent parameters to describe magnetite, the spinel phase in the Fe–O system (where there are 12 end-members).

When trying to combine the descriptions of the five simple spinels, a problem of consistency occurs due to different choices of reference for charge in the previously assessed systems. To be able to use parameters that are common in more than one simple spinel, e.g. $^oG_{Fe^{+2}:Fe^{+2}:Va:O^{-2}}$, it is required that the same value is used for that parameter in all descriptions. In the present case, different values had been used for $^oG_{Ni^{+2}:Ni^{+2}:Va:O^{-2}}$ and $^oG_{Cr^{+3}:Cr^{+3}:Va:O^{-2}}$ in the ternary systems. To be able to solve these inconsistencies a simplified model of a spinel solution with no vacancies, interstitials or divalent chromium is considered as a first approach: $(Fe^{+2}, Ni^{+2}, Cr^{+3}, Fe^{+3})_1(Fe^{+2}, Ni^{+2}, Cr^{+3}, Fe^{+3})_2 (O^{-2})_4$, see Fig. 1. This solution contains four simple spinels that are neutral: Fe_3O_4, $FeCr_2O_4$, $NiFe_2O_4$ and $NiCr_2O_4$. If all these spinels were normal spinels, the system could be described with $(Fe^{+2}, Ni^{+2})_1$ $(Cr^{+3}, Fe^{+3})_2(O)_4$, all compounds would be neutral and could be studied experimentally. Fig. 1 shows a schematic representation of the relations between the four simple spinels. All points on the neutral line between the normal and inverse spinels represent the stoichiometric compositions of Fe_3O_4, $FeCr_2O_4$, $NiFe_2O_4$ and $NiCr_2O_4$ denoted 23, 2C, N3 and NC, respectively, but with different distributions of divalent and trivalent ions on the two cation sublattices. Only one point on the line represents the equilibrium composition at a given temperature.

If the descriptions of the four simple spinels were to be merged and used in the same database, the reference points $^oG_{Fe^{+2}:Fe^{+2}:Va:O^{-2}}$, $^oG_{Ni^{+2}:Ni^{+2}:Va:O^{-2}}$, $^oG_{Cr^{+3}:Cr^{+3}:Va:O^{-2}}$ and $^oG_{Fe^{+3}:Fe^{+3}:Va:O^{-2}}$ (22, NN, CC and 33 from now on) must, of course, be the same in all descriptions. In this system with four simple spinels the Fe–O [17] and Cr–Ni–O [3] systems were assessed first. Those
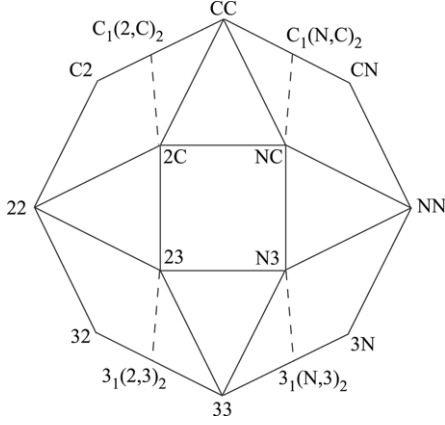
Fig. 1. Schematic figure of a spinel with four cations, two divalent and two trivalent, showing the relationship between the four simple spinels. The dashed lines represent the neutral lines. 2 stands for Fe^{+2}, 3 for Fe^{+3}, C for Cr^{+3} and N for Ni^{+2}. 22 stands for ${}^oG_{Fe^{+2}:Fe^{+2}:Va:O^{-2}}$, CC for ${}^oG_{Cr^{+3}:Cr^{+3}:Va:O^{-2}}$ and so on.

two systems have no common reference point and were assessed independently. The two remaining systems were assessed a few years later using the same reference points for 22 and 33 as [17] did, whereas NN and CC from [3] were not used, which led to that the assessment of the $NiCr_2O_4$ spinel is inconsistent with the other three. In the present work the Fe_3O_4, $FeCr_2O_4$ and $NiFe_2O_4$ spinels are accepted, so there is a need to take a closer look on the $NiCr_2O_4$ spinel, $(Cr^{+3}, Ni^{+2})_1(Cr^{+3}, Ni^{+2})_2 (O^{-2})_4$. The Gibbs energy for that spinel:

$$G_m = \sum_i \sum_j y'_i y''_j \, {}^oG_{ij} - TS_c + {}^EG_m \tag{13}$$

where the superscript $'$ and $''$ denote the first and second sublattice, respectively. The condition of electroneutrality gives:

$$2y'_N + 3y'_C + 2 \cdot 2y''_N + 2 \cdot 3y''_C = 8$$
$$y'_N = 1 - y'_C$$
$$y''_C = 1 - 0.5y'_C$$
$$y''_N = 0.5y'_C \tag{14}$$

where C and N denotes Cr^{+3} and Ni^{+2}, respectively.

Eqs. (13) and (14) give the following Gibbs energy expression:

$$\begin{aligned} G_m &= 0.5(1-y'_C)y'_C \, {}^oG_{NN} + (1-y'_C)(1-0.5y'_C) \, {}^o G_{NC} + 0.5y'^{\,2}_C \, {}^o G_{CN} \\ &\quad + y'_C(1-0.5y'_C) \, {}^oG_{CC} - TS_c + 0.5y'_C(1-y'_C)(1-0.5y'_C)L_{N:NC} \\ &\quad + 0.5y'^{\,2}_C(1-0.5y'_C)L_{C:NC} + 0.5y'^{\,2}_C(1-y'_C)L_{NC:N} \\ &\quad + y'_C(1-y'_C)(1-0.5y'_C)L_{NC:C}. \end{aligned} \tag{15}$$

The coefficient for each power of y'_C should be unchanged even if the individual parameters are changed. From Eq. (15) four sets of parameters are obtained:

$$y'^{\,0}_C : {}^o G_{NC} \tag{16}$$

$$y'^{\,1}_C : {}^oG_{NN} - 3\,{}^oG_{NC} + 2\,{}^oG_{CC} + L_{N:NC} + 2L_{NC:C} \tag{17}$$

$$y'^{\,2}_C : -2\,{}^oG_{NN} + 2\,{}^oG_{NC} + 2\,{}^oG_{CN} - 2\,{}^oG_{CC} - 3L_{N:NC}$$
$$\qquad + 2L_{C:NC} + 2L_{NC:N} - 6L_{NC:C} \tag{18}$$

$$y'^{\,3}_C : L_{N:NC} - L_{C:NC} - 2L_{NC:N} + 2L_{NC:C}. \tag{19}$$

From Eq. (16) it is seen that ${}^oG_{NC}$ could not be changed, which seems natural since that is the neutral compound. Since the Gibbs energy expression should be unchanged when the parameters change, Eqs. (17)–(19) lead to

$$2L_{NC:C}^{new} + L_{N:NC}^{new} = 2L_{NC:N}^{new} + L_{C:NC}^{new} \tag{20}$$

$$2L_{NC:C}^{new} + L_{N:NC}^{new} = {}^oG_{NN}^{old} - {}^oG_{NN}^{new} + 2\,{}^oG_{CC}^{old} - 2\,{}^oG_{CC}^{new} \tag{21}$$

$${}^oG_{CN}^{new} = {}^oG_{CN}^{old} + {}^oG_{CC}^{old} - {}^oG_{CC}^{new} - 0.5L_{C:NC}^{new} \tag{22}$$

where ${}^oG_{NN}^{old}$, ${}^oG_{CC}^{old}$ and ${}^oG_{CN}^{old}$ come from the assessment of Cr–Ni–O by [3], ${}^oG_{NN}^{new}$ from the assessment of Fe–Ni–O by [5] and ${}^oG_{CC}^{new}$ from the assessment of Cr–Fe–O by [4]. In the assessment of Cr–Ni–O all $L^{old} = 0$. The parameters ${}^oG_{CN}^{new}$, $L_{NC:C}^{new}$, $L_{N:NC}^{new}$, $2L_{NC:N}^{new}$ and $L_{C:NC}^{new}$ should be given such values that the above conditions are satisfied. There are three equations, (20)–(22), and five unknown parameters, $L_{NC:C}^{new}$, $L_{N:NC}^{new}$, $L_{NC:N}^{new}$, $L_{C:NC}^{new}$ and ${}^oG_{CN}^{new}$, so two of the new parameters can be given arbitrary values. On the neutral line all such sets of parameter values will give the same result. For the $NiCr_2O_4$ spinel the following parameters are chosen:

$${}^0G_{NC}^{new} = {}^0G_{NC}^{old} \tag{23}$$

$${}^0G_{CN}^{new} = {}^0G_{CN}^{old} + {}^0G_{CC}^{old} - {}^0G_{CC}^{new} \tag{24}$$

$${}^0G_{NN}^{new} \quad \text{from [5]} \tag{25}$$

$${}^0G_{CC}^{new} \quad \text{from [4]} \tag{26}$$

$$L_{N:NC} = L_{C:NC} = 0 \tag{27}$$

$$L_{NC:N} = L_{NC:C} = {}^0G_{CC}^{old} - {}^0G_{CC}^{new} + 0.5\,{}^0G_{NN}^{old} - 0.5\,{}^0G_{NN}^{new}. \tag{28}$$

The calculated properties of the $NiCr_2O_4$ spinel, which was primarily assessed assuming $\Delta\,{}^0G_{NC:NC} = L_{N:NC} = L_{C:NC} = L_{NC:N} = L_{NC:C} = 0$, are unaffected by this change in parameter values and the reference points NN and CC are now consistent in the four systems considered. However, extrapolations to higher order system are affected by this change in parameter values.

Up till now the influence of vacancies have not been considered. To model oxygen excess, vacancies are introduced on the octahedral sublattice. In the previous assessments of Fe_3O_4, $FeCr_2O_4$ and $NiFe_2O_4$ the spinel phases were modelled with vacancies on the octahedral sublattice, while the $NiCr_2O_4$ spinel was modelled as a stoichiometric phase. In the present work, with the different descriptions merged, the $NiCr_2O_4$ spinel will contain vacancies since ${}^oG_{Ni^{+2}:Va:Va:O^{-2}}$, ${}^oG_{Cr^{+2}:Va:Va:O^{-2}}$ and ${}^oG_{Cr^{+3}:Va:Va:O^{-2}}$ are introduced from the other descriptions. However, the influence on the phase relations are negligible and no reassessment was considered necessary.

According to the description of Fe–O, substitution of a vacancy for a Fe^{+2} ion on the third sublattice requires an energy change of $2G + D - B$ in magnetite. It is assumed to be independent of the ions on the other sublattices, thus the same energy change is used for substitution of a vacancy for a Fe^{+2} ion on the third sublattice also in the other spinel systems; $FeCr_2O_4$, Cr_3O_4, $NiFe_2O_4$ and $NiCr_2O_4$. As mentioned earlier the introduction of Cr^{+2} on the interstitial sublattice was necessary for the modelling of the diffusivities. The same energy change as for substituting a vacancy for a Fe^{+2} ion was adopted for the substitution of a vacancy for a Cr^{+2} ion. This addition to the spinel phase did not require any reassessment since the influence on the phase relations of the systems appeared to be negligible.

Substitution of a Cr^{+3} for a Cr^{+2} on the first sublattice requires an energy change of S, evaluated in the Cr–Fe–O assessment [4]. For completeness in the database, this energy change is assumed to be independent of the ions on the other sublattices and is used also for the remaining spinel systems.

Fe_3O_4, $FeCr_2O_4$ and $NiFe_2O_4$ have magnetic transitions which are modelled using Eq. (3). The values for the assessed Curie temperature and Bohr magneton number are found in Table 1.

The value of 858 K for the Fe–Ni spinel may seem strange, since $NiFe_2O_4$ has a magnetic transition at 853 K. This is due to the inverse nature of $NiFe_2O_4$. The Gibbs energy of $NiFe_2O_4$ is approximately equal to $0.5\,{}^oG_{Fe^{+3}:Fe^{+3}:Va:O^{-2}} + 0.5\,{}^oG_{Fe^{+3}:Ni^{+2}:Va:O^{-2}}$, where the Curie temperature of each compound is 848 and 858 K, respectively. To model the Bohr magneton number for $NiFe_2O_4$ all end-members containing Ni was given the value zero, and an excess value was optimised. To be able to get a value of less than $3.18 (= (0.5\beta_{Fe^{+3}:Fe^{+3}:Va:O^{-2}} + 0.5\beta_{Fe^{+3}:Ni^{+2}:Va:O^{-2}})/7)$ for the Bohr magneton number of $NiFe_2O_4$, a negative value for the excess parameter is needed.

Table 1
Magnetic properties of the spinel phase

Compounds	Curie temperature (K)	Bohr magneton number
Only Fe	848	44.54
Only Cr or Cr + Fe	100	0.9
Only Ni or Fe + Ni	858	0
$Fe^{+3} : Fe^{+3}, Ni^{+2} :$ Va $: O^{-2}$	0	-69.61
All other compounds	0	0

2.6. Solid solution phases (bcc and fcc)

In the present study, it was assumed that oxygen dissolves interstitially. Previously, for example [17,21], this solubility was modelled to be substitutional which is probably more physically correct. However, it has now been decided to conform to the majority of descriptions of oxygen in metallic phases, i.e. interstitially dissolved. The bcc and fcc phases are described using a two-sublattice model with metal atoms on the first sublattice and vacancies and oxygen on the second sublattice. The number of interstitial sites in the bcc and fcc phases are 3 and 1, respectively:

bcc: $(Cr, Fe, Ni)_1 (O, Va)_3$

fcc: $(Cr, Fe, Ni)_1 (O, Va)_1$.
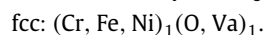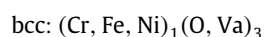
The magnetic properties of bcc and fcc were described using the model in Section 2.1.

2.7. Gas

The gas phase is described as an ideal gas containing the species Cr, CrO, CrO_2, CrO_3, Cr_2, Cr_2O, Cr_2O_2, Cr_2O_3, Fe, FeO, FeO_2, Fe_2, Ni, NiO, Ni_2, O, O_2 and O_3 [22].

2.8. Sigma phase

The sigma phase is the only phase for which no oxygen solubility has been modelled, and will therefore not be further discussed.

3. Results and discussion

3.1. Unary and binary data

Data for the pure elements were taken from [23]. Data for the binary systems were taken from existing assessments, see Table 2, except for Cr–O and Fe–O which were slightly changed in this work. The calculated phase diagrams for all binary systems are shown in Figs. 2–8.

3.1.1. Cr–O

The binary Cr–O system has been reassessed later by [28] using the same models as [3], but with both Cr^{+2} and Cr^{+3} species in the liquid phase. However, their assessment is not considered in this work. In the assessment by [3], two drawbacks are found. First, the miscibility gap in the liquid phase does not close with increasing temperature. Second, the Cr_3O_4 phase was first modelled as a stoichiometric phase [3], but in their later work with the Cr–Fe–O system [4], Cr_3O_4 was incorporated in the model for the spinel phase, thus including Cr^{+3} on tetrahedral sites and vacancies on octahedral sites. This led to a change in the melting temperature of Cr_3O_4 that deviated from the experimental data and the liquid phase was therefore reassessed. Using the experimental information from [29,30] resulted in the phase diagram shown in Fig. 4. A comparison with the phase diagram calculated by [4] and experimental information is presented in Fig. 5.
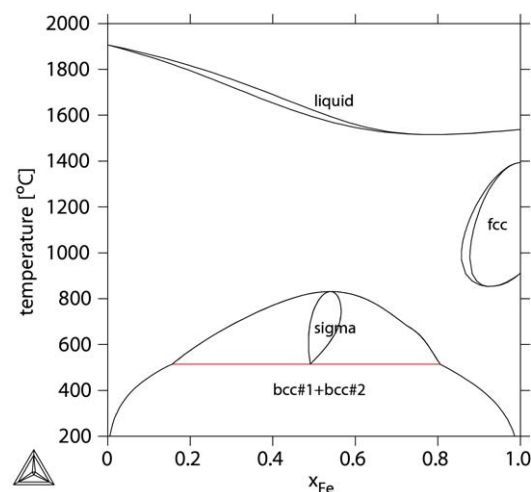
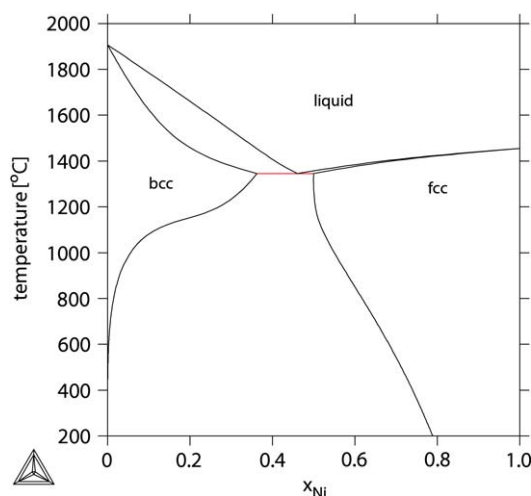**Fig. 2.** Calculated Cr–Fe phase diagram.

Fig. 3. Calculated Cr–Ni phase diagram.

3.1.2. Fe–O

In the Fe–O system, hematite has been modified with an interstitial sublattice to enable deviation from stoichiometry, see discussion in Section 2.4. Hematite is calculated to be stable down to $x_O = 0.5999$ at 1200 °C, in agreement with experiments [31].

3.1.3. Fe–Ni

In the Fe–Ni binary there is at low temperatures an ordered fcc phase, $L1_2$, located at Ni_3Fe. With a four sublattice model, both the disordered A1 phase and the ordered $L1_0$ and $L1_2$ phases could be described using the same Gibbs energy expression. However, this ordered phase is of no interest for steels, thus not considered in this work.

3.2. Ternary systems

Data for the four ternary subsystems were taken from existing assessments, see Table 3. The oxygen containing systems have been slightly modified in this work. For the metallic system, Cr–Fe–Ni, the assessment by [6,7] is accepted.

3.2.1. Cr–Fe–O

The assessment of the Cr–Fe–O system has been performed by [4]. The liquid phase has been reassessed in this work due to an unwanted miscibility gap discovered at increasing temperature,

Table 2
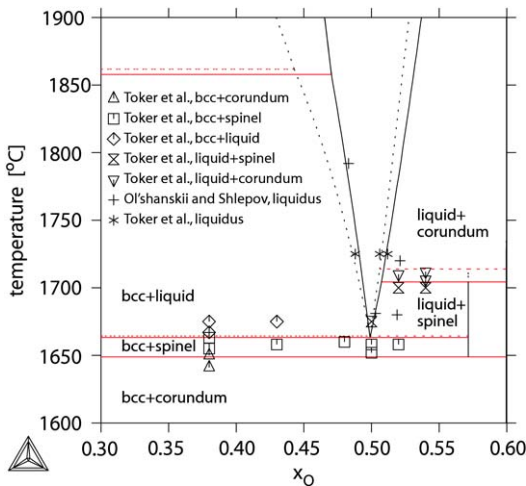References for assessed binary systems used in this work

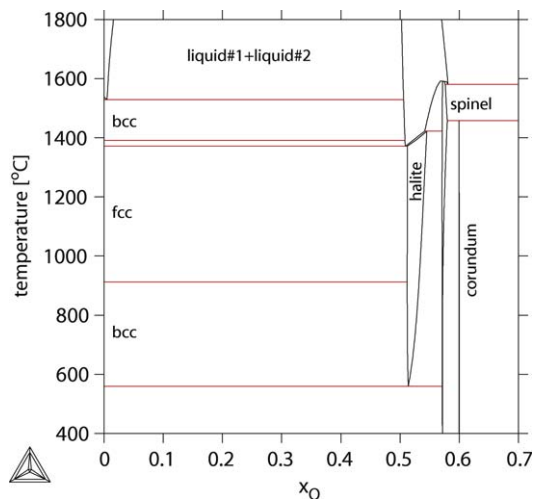| System	Reference
Cr–Fe	Andersson and Sundman [24], Lee [7]
Cr–Ni	Dinsdale and Chart [25], Lee [7]
Cr–O	Taylor and Dinsdale [3,4], Kowalski and Spencer [26], this work
Fe–Ni	Dinsdale and Chart [27], Lee [7]
Fe–O	Sundman [17], Selleby and Sundman [18], Kowalski and Spencer [26], this work
Ni–O	Taylor and Dinsdale [3], Kowalski and Spencer [26]
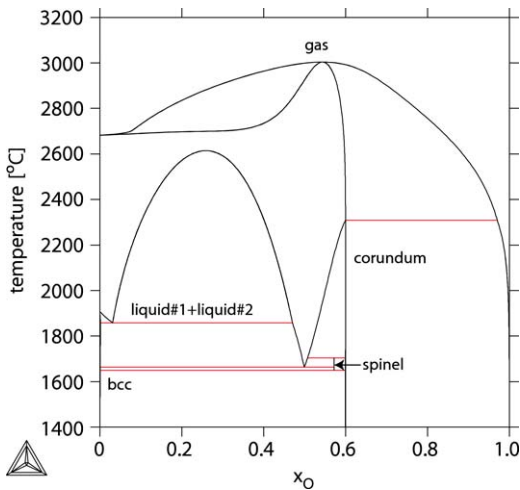
Fig. 4. Calculated Cr–O phase diagram.
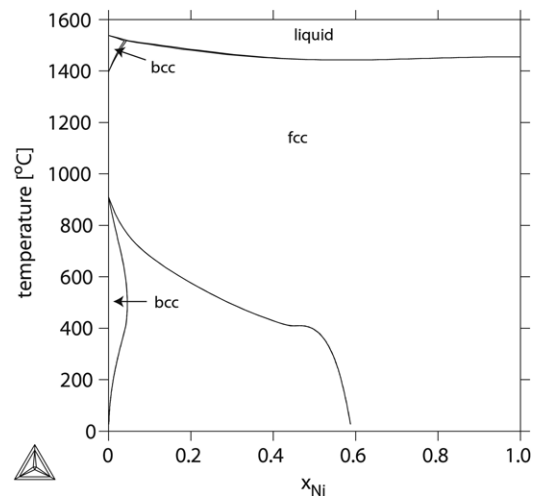
Fig. 6. Calculated Fe–Ni phase diagram.

Fig. 5. Calculated and experimental [29,30] Cr–O phase diagram. Dashed line from [4], solid line this work.

Fig. 7. Calculated Fe–O phase diagram.

Table 3
References for assessed ternary systems used in this work

System	Reference
Cr–Fe–Ni	Lee [6,7]
Cr–Fe–O	Taylor and Dinsdale [4], this work
Cr–Ni–O	Taylor and Dinsdale [3], this work
Fe–Ni–O	Luoma [5], this work

see Fig. 9. Such miscibility gap is much easier to find nowadays with modern software, and the description by [4] aimed to cover the temperature range 298 K to about 2600 K. The miscibility gap arises due to the rather large temperature dependency on the assessed reciprocal interaction terms. As a first step, since almost all experimental information regarding the liquid phase concerns measurements at 1600 °C, all parameters from [4] were

recalculated for that temperature. The calculated melting point of the spinel phase in air at 1 atmosphere compared to [4] was now 50 °C lower than the old description. A large part of this difference is however due to the introduction of the neutral $FeO_{1.5}$ species. ([4] modelled the liquid phase using the ionic two-sublattice model with the charged Fe^{+3} species.) The parameter $L_{Cr^{+3},Fe^{+2}:O^{-2}}$ was then adjusted to give the correct melting point of the spinel phase under the conditions used in Fig. 9, but still keep the same values on all ternary parameters as [4] at 1600 °C. With this minor change in parameters all figures concerning the liquid phase presented by [4] could be reproduced within the experimental scatter.

Some calculated equilibria are presented in Table 4 together with available experimental information and the calculated results from [4]. [4] used the data from [32] to assess the temperature dependence, who measured the solubility of oxygen in Cr–Fe in equilibrium with solid oxide phases at different temperatures. The
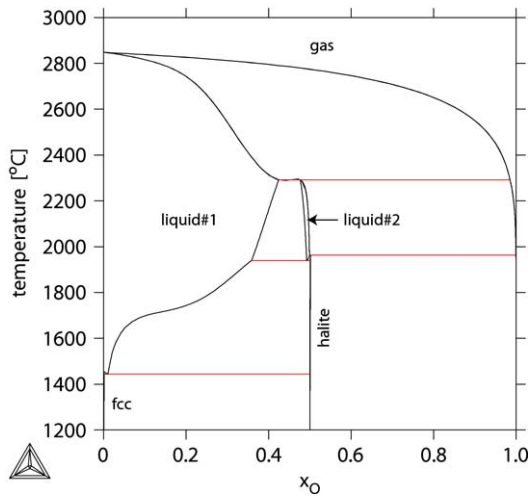
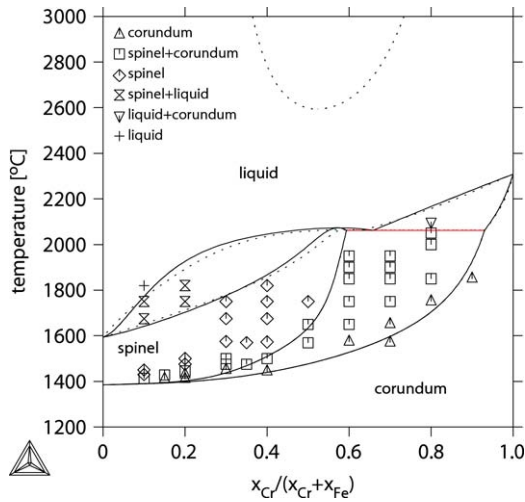**Fig. 8.** Calculated Ni–O phase diagram.

Fig. 9. Calculated and experimental [33] phase diagram of Cr–Fe–O in air at 1 atm. Dashed line from [4], solid line this work.
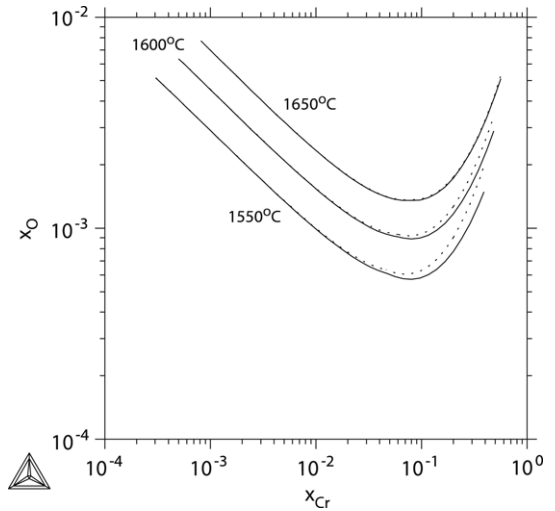

Fig. 10. Calculated solubility of oxygen in liquid Fe–Cr. Dashed line from [4], solid line this work.
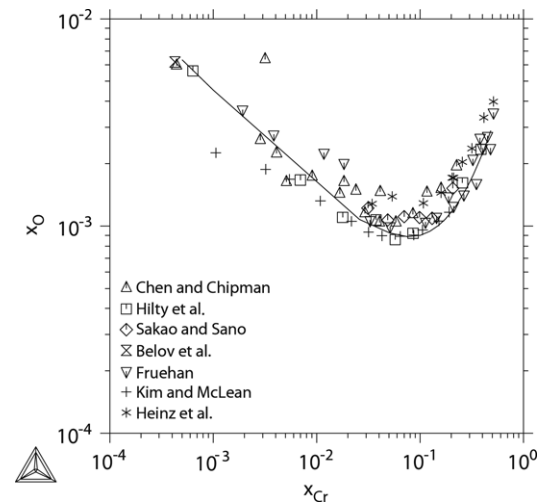

Fig. 11. Calculated and experimental [34–36,40,41,38,32] solubility of oxygen in liquid Fe–Cr at 1600 °C.
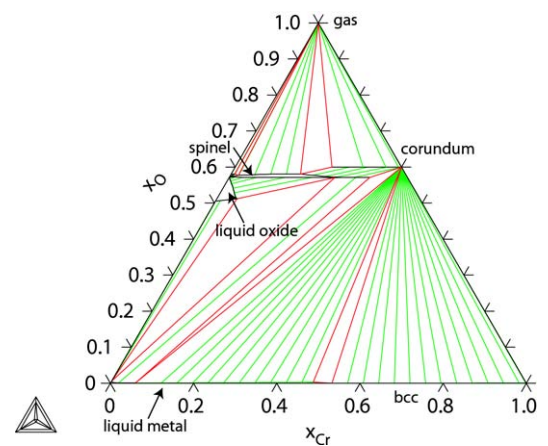

Fig. 12. Calculated isothermal section of the Cr–Fe–O system at 1600 °C.

calculated solubility of oxygen for three different temperatures is shown in Fig. 10 using both the parameters from the present work and [4]. In Fig. 11 the calculated oxygen solubility together with experimental data is shown. The rather scattered experimental values and the small difference between this description and [4] do not motivate the large temperature dependence used by [4] for the reciprocal interaction terms.

In the model for the spinel phase, Cr^{+2} has been introduced to the third sublattice, normally filled mainly with vacancies. An isothermal section of the system at 1600 °C is shown in Fig. 12.

3.2.2. Cr–Ni–O

The assessment of the Cr–Ni–O system has been performed by [3]. The same situation with an unwanted miscibility gap in the liquid phase was found also in this system, see Fig. 13. The liquid phase has therefore been reassessed in this work, but using the same experimental information as [3].

The solubility of oxygen in molten Cr–Ni at various temperatures has been studied by [32,42,43]. The calculated oxygen solubility in equilibrium with corundum at 1600 °C is shown in Fig. 14 together with experiments and the calculation by [3]. The values from [43] are in poor agreement with the others at a Cr-content below ≈10%. [43] identified the stable phase to be $NiCr_2O_4$ below 6 mass-% Cr and Cr_2O_3 at higher Cr-contents. Above ≈0.01% Cr the

calculated stable phase is Cr_2O_3, and below $NiCr_2O_4$. The values reported by [32] could not be reproduced with the current model. To reproduce those values corundum would have to be more stable. [32,42,44] measured oxygen activities, shown in Fig. 15.

Table 4
Comparison between this work, [4] and experimental information

Composition of liquid metal in equilibrium with spinel and Cr_2O_3 at 1600 °C (see three-phase triangle in Fig. 12):

Reference	[34]	[35]	[36]	[37]	[29]	[38]	[32]	[4]	This work
mass-% Cr	5.5	9[a]	9[a]	7	5.85	3[a]	5	5.60	5.60

Compositions and oxygen partial pressure for the three-phase equilibrium between liquid metal, Fe-rich liquid oxide and spinel at 1600 °C (see three-phase triangle in Fig. 12):

Reference	[39]	[29]	[4]	This work
x_{Cr} liq. metal	0.000428	0.00055	0.00050	0.00050
x_O liq. metal	0.00625	–	0.00632	0.00636
u_{Cr} liq. oxide	0.162	≈0.1	0.099	0.099
u_{Cr} spinel	–	0.602	0.592	0.592
$\log(p_{O_2})$	–	−8.3 ± 0.25	−8.30	−8.30

Compositions (u_{Cr}) and oxygen partial pressure for the three-phase equilibrium between liquid metal, Cr-rich liquid oxide and spinel at 1750 °C:

Reference	[29]	[4]	This work
Liq. metal	0.517	0.502	0.493
Liq. oxide	–	0.962	0.960
Spinel	0.978	0.967	0.965
$\log(p_{O_2})$	−10.19	−10.10	−10.06

Compositions (u_{Cr}) and oxygen partial pressure for the three-phase equilibrium between liquid metal, Cr-rich liquid oxide and spinel at 1825 °C:

Reference	[29]	[4]	This work
Liq. metal	0.188	0.305	0.272
Liq. oxide	–	0.928	0.915
Spinel	0.932	0.930	0.919
$\log(p_{O_2})$	−8.87	−9.10	−9.01

$u_{Cr} = x_{Cr}/(x_{Cr} + x_{Fe})$.
[a] Cr_3O_4 found to be the stable oxide instead of Cr_2O_3.
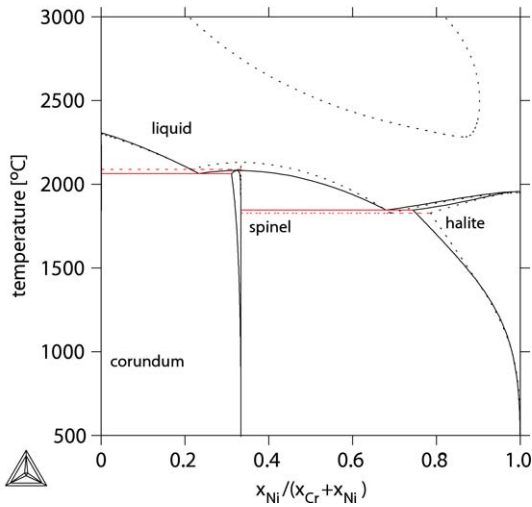
Fig. 13. Calculated phase diagram of Cr–Ni–O in air at 1 atm. Dashed line from [3], solid line this work.

Fig. 14. Calculated and experimental [32,42,43] solubility of oxygen in liquid Cr–Ni at 1600 °C. Dashed line from [3], solid line this work.

The description of the spinel phase, $NiCr_2O_4$, was modified but without any reassessment, see Section 2.5. The melting point of $NiCr_2O_4$ is now calculated to be 2083 °C compared to 2138 °C calculated by [3] due to the reassessment of the liquid phase.

The solubility of Cr in wustite was modelled by [4] in the Cr–Fe–O assessment using the unary compound $G_{Cr^{+3}:O^{-2}}$. Unfortunately, this was not the same value that they used earlier to describe the solubility of Cr in bunsenite. In the present work the value for $G_{Cr^{+3}:O^{-2}}$ from the Cr–Fe–O assessment was adopted and an interaction parameter, $L_{Cr^{+3},Ni^{+2}:O^{-2}}$, was introduced to be able to reproduce the solubility of Cr in bunsenite. The solubility of Cr in bunsenite is shown in Fig. 16 in comparison with previous assessment and experimental data. The fit to the rather scattered experimental data is good. An isothermal section of the phase diagram at 1600 °C is shown in Fig. 17.
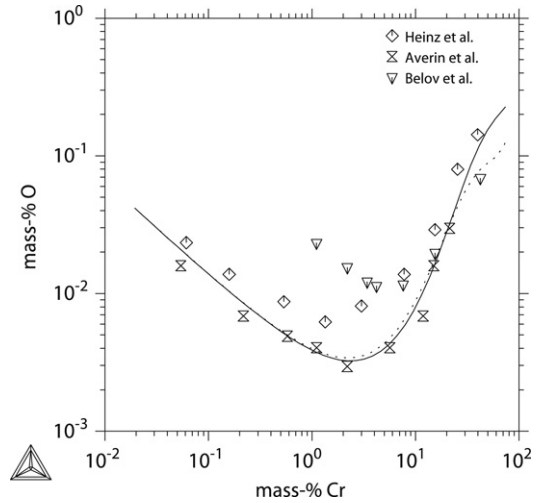
3.2.3. Fe–Ni–O

The assessment of the Fe–Ni–O system has been performed by [5]. The spinel phase in the Fe–Ni–O system has been reassessed in this work. In the assessment by [5], the magnetic contribution to Gibbs energy was not modelled using the model described in Section 2.1. To model the λ-shaped heat capacity curve, [5] used two functions to describe Gibbs energy: one function that was valid at temperatures below the magnetic transition and one function at temperatures above the magnetic transition. The magnetic contribution to the spinel phase is now described using the same model for all compounds. In Fig. 18, the heat capacity of $NiFe_2O_4$ in comparison with previous assessment and experimental data is shown, and in Fig. 19 the enthalpy.

The cation distribution of $NiFe_2O_4$ has been studied by [49] at various temperatures. $NiFe_2O_4$ is almost a complete inverse spinel. The calculated degree of inversion is shown in Fig. 20. In Fig. 21, calculated oxygen activity at 1000 °C in the spinel area is
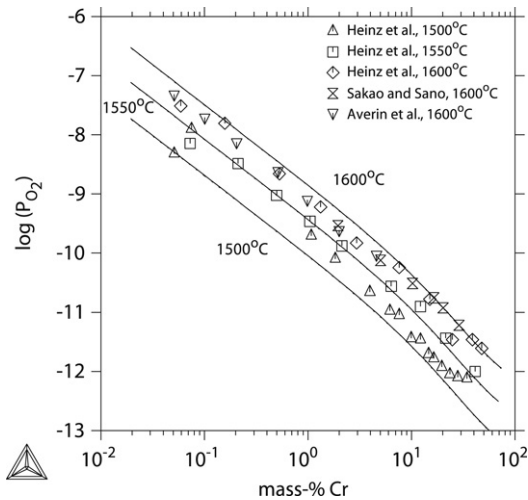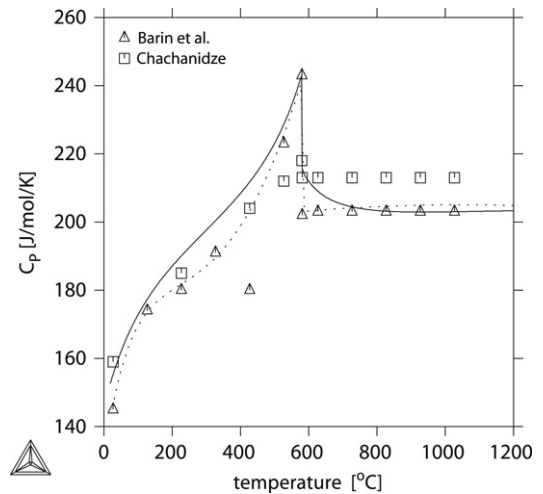
Fig. 15. Calculated and experimental [32,44,42] values of oxygen partial pressures at various temperatures. Dashed line from [3], solid line this work (the difference is very small and can not be distinguished in this figure).
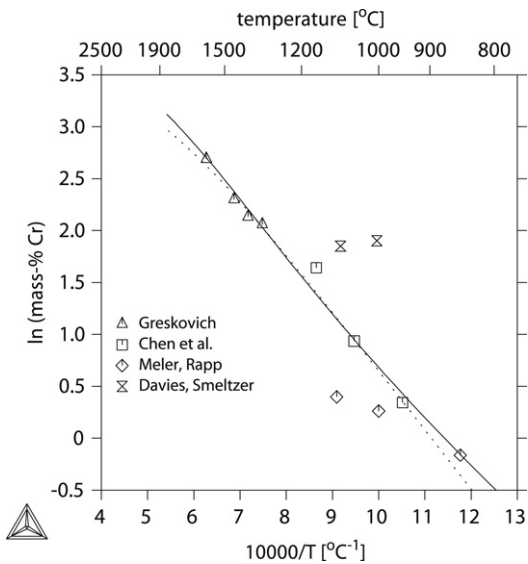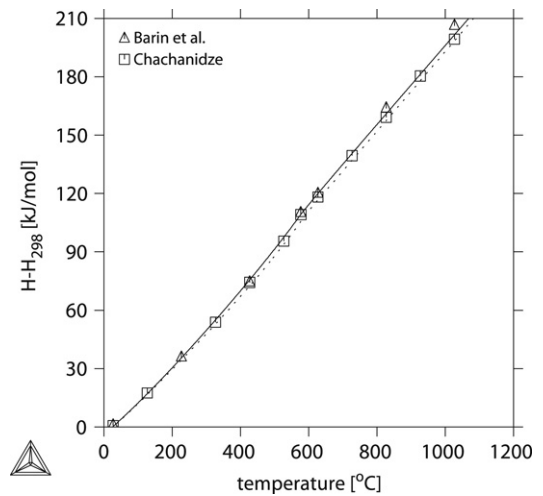

Fig. 16. Calculated and experimental [45–48] solubility of Cr in NiO. Dashed line from [3], solid line this work.
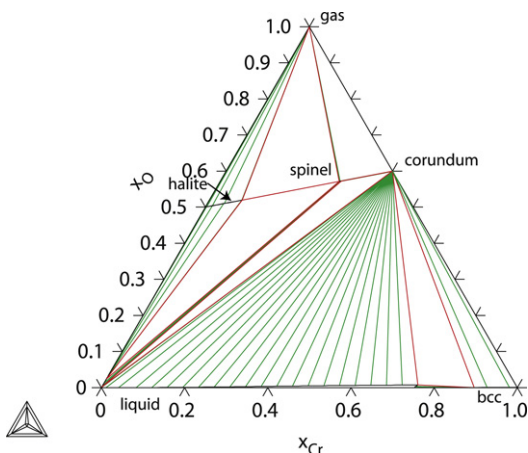
Fig. 17. Calculated isothermal section of the Cr–Ni–O system at 1600 °C.

Fig. 18. Calculated and experimental [50,51] heat capacity of NiFe$_2$O$_4$. Dashed line from [5], solid line this work.

Fig. 19. Calculated and experimental [50,51] enthalpy of NiFe$_2$O$_4$. Dashed line from [5], solid line this work.

shown with experimental data. An isothermal section of the phase diagram at 1600 °C is shown in Fig. 22. The calculated Fe$_2$O$_3$–NiO section is shown in Fig. 23.

3.3. Quaternary system, Cr–Fe–Ni–O

There are only a few experiments concerning the quaternary system. [32,61] measured the solubility of oxygen in molten Cr–Fe alloys with different Ni-contents at 1550 and 1600 °C respectively. Their studies gave similar results; increasing the Ni-content will decrease the solubility of oxygen in the alloys. The experimental data are quite well reproduced without using any quaternary parameters, see Figs. 24 and 25.

[62] investigated the solid solution behaviour of the binary Ni(Fe$_{1-n}$Cr$_n$)$_2$O$_4$ spinel. The existence of two spinel phases was detected using both energy dispersive X-ray spectrometry (EDX) and electron microprobe analyses (EMPA). They estimated the consolute solution temperature to about 750 °C at $n \approx 0.5$. The solvus becomes increasingly asymmetric at lower temperatures. In the present work the parameters $L_{Fe^{+3},Ni^{+2}:Cr^{+3}}$ and $L_{Fe^{+3}:Cr^{+3},Ni^{+2}}$ were adjusted to give the miscibility gap shown in Fig. 26.

At low temperatures NiFe$_2$O$_4$ is an inverse spinel with few Fe^{+2} ions on the tetrahedral site. Addition of Cr, which has a strong octahedral site preference, substitutes Fe^{+3} ions to give an almost
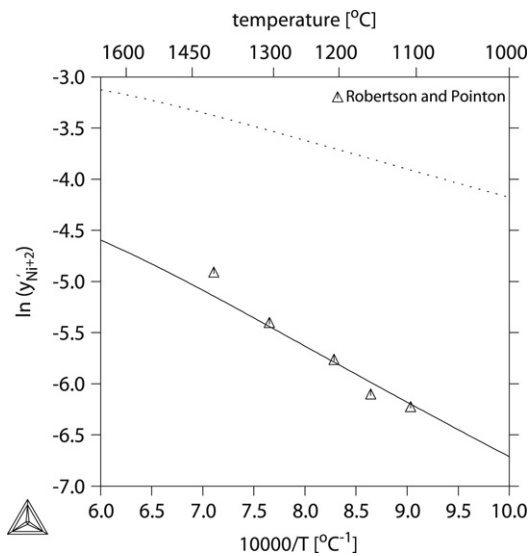
Fig. 20. Calculated and experimental [49] degree of inversion in $NiFe_2O_4$. Dashed line from [5], solid line this work.
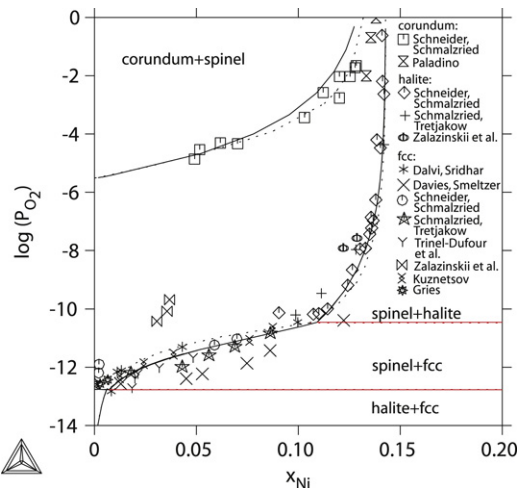
Fig. 21. Calculated and experimental [52–60] oxygen activity. Dashed line from [5], solid line this work.
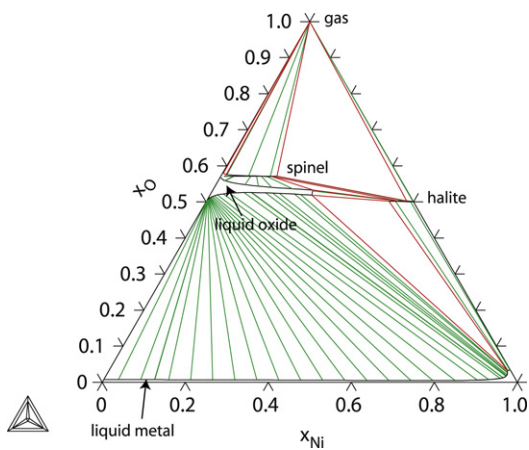
Fig. 22. Calculated isothermal section of the Fe–Ni–O system at 1600 °C.

Fig. 23. Calculated phase diagram of Fe–Ni–O in air at 1 atm. Dashed line from [5], solid line this work.

Fig. 24. Calculated and experimental [32] solubility of oxygen in Cr–Fe–Ni alloys at 1550 °C.
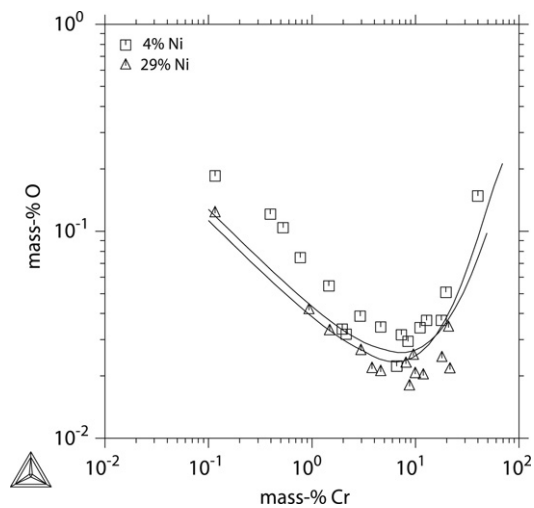
Fig. 25. Calculated and experimental [61] solubility of oxygen in Cr–Fe–Ni alloys at 1600 °C.

normal spinel at the $NiCr_2O_4$ composition. According to [62] initial substitution of Cr^{+3} ions for Fe^{+3} ions is expected to occur only on Fe^{+3} ions located in octahedral sites. Substitution of Cr^{+3} ions for Fe^{+3} ions on tetrahedral sites will not take place until n reaches

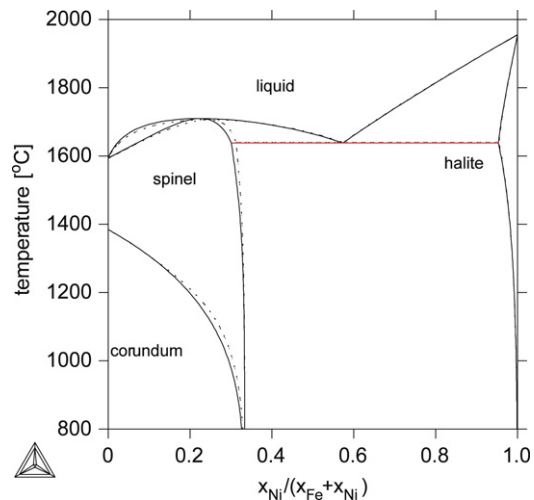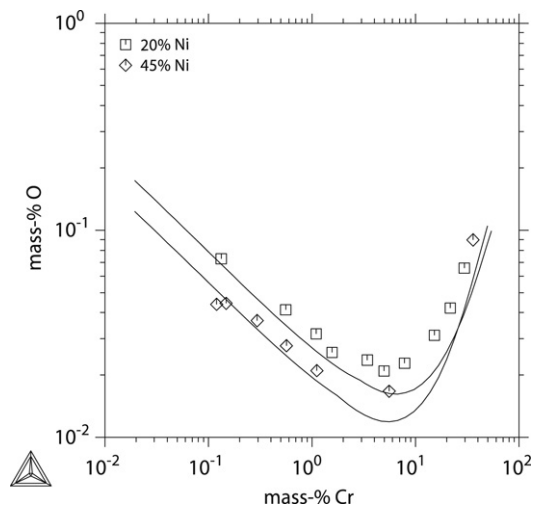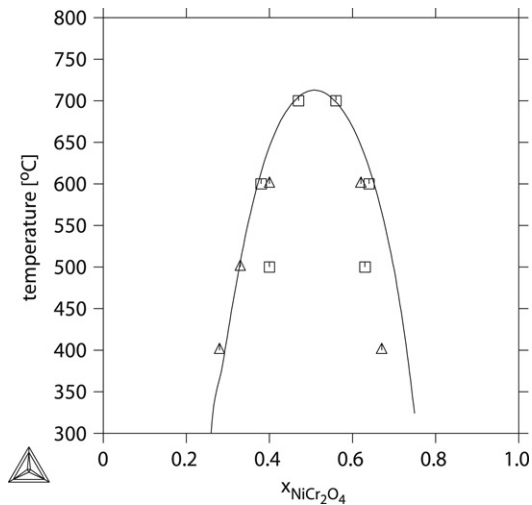**Fig. 26.** Calculated and experimental [62] miscibility gap in the $NiCr_2O_4$– $NiFe_2O_4$ spinel binary.

Fig. 28. Calculated oxide scale formed on a stainless steel (Fe–18Cr–8Ni mass-%) at 1000 °C.
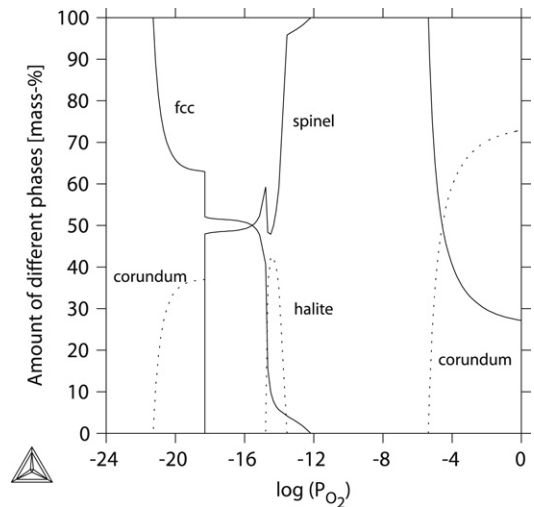

Fig. 27. Calculated distribution of ions at 727 °C when the spinel composition changes from $NiFe_2O_4$ to $NiCr_2O_4$.

Fig. 29. Calculated composition of oxides for the steel in Fig. 28.

0.5 and all of the Fe^{+3} ions that were originally on octahedral sites have been replaced. The calculated cation distribution at 727 °C is shown in Fig. 27, where this tendency is reproduced. At higher temperature the cation distribution becomes more random.
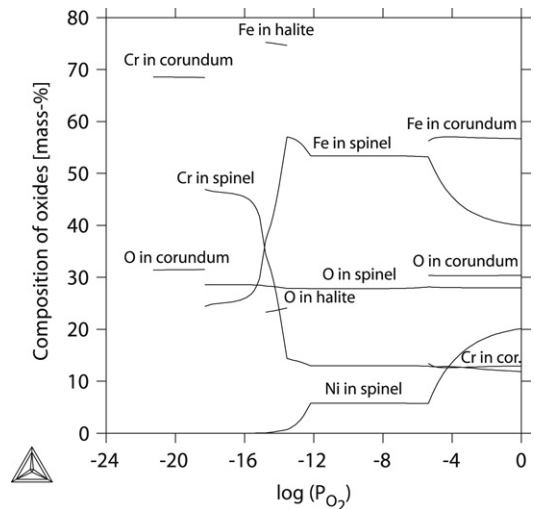
The thermodynamic description presented in this work can be used to predict the oxidation behaviour of a Cr–Ni steel. Figs. 28 and 29 show a calculation of an oxide scale formation on an 18/8 stainless steel. In Fig. 28 the different phases formed are shown and in Fig. 29 the composition of the phases. However, for a more accurate calculation the DICTRA software [63], together with the thermodynamic database presented in this work and an accurate kinetic database, should be used to simulate the oxide scale formation.

4. Conclusions

In the present work, a thermodynamic description of the Cr–Fe–Ni–O system is presented. A complete list of all parameters is found in Table 5. All binary and higher order systems are thoroughly studied and revised where necessary. The liquid phase in the Cr–Fe–O and Cr–Ni–O systems was reassessed due to unwanted miscibility gaps found in the previous assessments at high temperatures. In the model of the corundum phase iron was

added to an interstitial sublattice to be able to model diffusion in hematite. When two or more assessments are merged to be used in the same database, inconsistencies could be found even though the same model has been used. This was the case for the halite and spinel phases in the present work. To solve the inconsistency in the halite phase an interaction parameter was optimised. The inconsistency of the spinel phase was due to different choices of reference for charge, resulting in deviant values for some of the end-members common in more than one system. The spinel phase was made consistent without any reassessment, by a procedure with the introduction of interaction parameters. The calculated properties of the simple spinels (Cr_3O_4, Fe_3O_4, $FeCr_2O_4$, $NiFe_2O_4$ and $NiCr_2O_4$) are unaffected by the change of parameter values.

Apart from describing the miscibility gap in the $NiCr_2O_4$– $NiFe_2O_4$ spinel, no quaternary parameters are used in the Cr–Fe–Ni–O system. The description of the liquid phase in the quaternary system is obtained only by extrapolation of the ternary systems and the agreement with the limited experimental data on the quaternary system is quite good.

Table 5
Parameters for the Cr–Fe–Ni–O system (in SI units; J, mol, K)

Liquid: $(Cr^{3+}, Fe^{2+}, Ni^{2+})_P (O^{2-}, FeO_{1.5}, Va^{-Q})_Q$

$$^0G_{Cr+3:O-2} - 2H_{Cr}^{SER} - 3H_O^{SER} = 2GCRLIQ + 1.5GO2GAS - 1\,047\,074 + 260.777\,T - 3.97112\,T\ln T$$

$$^0G_{Fe+2:O-2} - 2H_{Fe}^{SER} - 2H_O^{SER} = 4GFEOLIQ$$

$$^0G_{Ni+2:O-2} - 2H_{Ni}^{SER} - 2H_O^{SER} = 2GNILIQ + GO2GAS - 402\,345.6 + 176.606\,T - 4.35796\,T\ln T$$

$$^0G_{Cr+3:Va} - H_{Cr}^{SER} = GCRLIQ$$

$$^0G_{Fe+2:Va}\, H_{Fe}^{SER} = GFELIQ$$

$$^0G_{FeO_{1.5}} - H_{Fe}^{SER} - 1.5H_O^{SER} = 2.5GFEOLIQ - 89\,819 + 39.962\,T$$

$$^0G_{Ni+2:Va} - H_{Ni}^{SER} = GNILIQ$$

$$^0L_{Cr+3,Fe+2:O-2} = -60\,000 + 38.3\,T^a$$

$$^1L_{Cr+3,Fe+2:O-2} = 8650^a$$

$$^2L_{Cr+3,Fe+2:O-2} = -12\,975^a$$

$$^0L_{Cr+3,Ni+2:O-2} = 60\,000 - 49.1\,T^a$$

$$^0L_{Cr+3,Fe+2:Va} = -17\,737 + 7.996546\,T$$

$$^1L_{Cr+3,Fe+2:Va} = -1331$$

$$^0L_{Cr+3,Ni+2:Va} = 318 - 7.3318\,T$$

$$^1L_{Cr+3,Ni+2:Va} = 16\,941 - 6.3696\,T$$

$$^0L_{Fe+2,Ni+2:Va} = -16\,911 + 5.1622\,T$$

$$^1L_{Fe+2,Ni+2:Va} = 10\,180 - 4.146656\,T$$

$$^0L_{Cr+3,Fe+2,Ni+2:Va} = 36\,583$$

$$^1L_{Cr+3,Fe+2,Ni+2:Va} = 13\,254$$

$$^2L_{Cr+3,Fe+2,Ni+2:Va} = -10\,018$$

$$^0L_{Cr+3:O-2,Va} = 280\,000 - 99.3\,T^a$$

$$^1L_{Cr+3:O-2,Va} = -146\,000^a$$

$$^2L_{Cr+3:O-2,Va} = -65\,000^a$$

$$^0L_{Fe+2:O-2,Va} = 176\,681 - 16.368\,T$$

$$^1L_{Fe+2:O-2,Va} = -65\,655 + 30.869\,T$$

$$^0L_{Ni+2:O-2,Va} = 176\,711 - 50.2286\,T$$

$$^1L_{Ni+2:O-2,Va} = 22\,914.8$$

$$^2L_{Ni+2:O-2,Va} = 42\,079.6$$

$$^0L_{Fe+2:O-2,FeO_{1.5}} = -26\,362$$

$$^1L_{Fe+2:O-2,FeO_{1.5}} = 13\,353$$

$$^0L_{Cr+3:FeO_{1.5},Va} = 110\,000^a$$

$$^0L_{Fe+2:FeO_{1.5},Va} = 110\,000$$

$$^0L_{Ni+2:FeO_{1.5},Va} = 110\,000^a$$

$$^0L_{Cr+3,Fe+2:O-2,Va} = -61\,730^a$$

$$^1L_{Cr+3,Fe+2:O-2,Va} = -8650^a$$

$$^2L_{Cr+3,Fe+2:O-2,Va} = 12\,975^a$$

$$^0L_{Cr+3,Ni+2:O-2,Va} = -340\,000^a$$

$$^2L_{Cr+3,Ni+2:O-2,Va} = 240\,000^a$$

$$^0L_{Fe+2,Ni+2:O-2,Va} = -69\,412.057$$

$$^1L_{Fe+2,Ni+2:O-2,Va} = 71\,409.34$$

$$^2L_{Fe+2,Ni+2:O-2,Va} = 10\,202.34$$

$GCRLIQ\,(298.15 < T < 2180) = 24\,339.955 - 11.420225\,T + 2.37615E - 21\,T^7 + GHSERCR$

$GCRLIQ\,(2180 < T < 6000) = -16\,459.984 + 335.616316\,T - 50\,T\ln T$

$GFELIQ\,(298.15 < T < 1811) = 12\,040.17 - 6.55843\,T - 3.6751551E - 21\,T^7 + GHSERFE$

$GFELIQ\,(1811 < T < 6000) = -10\,838.83 + 291.302\,T - 46\,T\ln T$

$GNILIQ\,(298.15 < T < 1728) = 16\,414.686 - 9.397\,T - 3.82318E - 21\,T^7 + GHSERNI$

$GNILIQ\,(1728 < T < 6000) = 18\,290.88 - 10.537\,T - 1.12754E + 31/T^9 + GHSERNI$

$GFEOLIQ = -137\,252 + 224.641\,T - 37.1815\,T\ln T$

$GHSERCR\,(298.15 < T < 2180) = -8856.94 + 157.48\,T - 26.908\,T\ln T + 0.00189435\,T^2 - 1.47721E - 06\,T^3 + 139\,250/T$

$GHSERCR\,(2180 < T < 6000) = -34\,869.344 + 344.18\,T - 50\,T\ln T - 2.88526E + 32/T^9$

$GHSERFE\,(298.15 < T < 1811) = 1225.7 + 124.134\,T - 23.5143\,T\ln T - 0.00439752\,T^2 - 5.8927E - 08\,T^3 + 77359/T$

$GHSERFE\,(1811 < T < 6000) = -25\,383.581 + 299.31255\,T - 46\,T\ln T + 2.29603E + 31/T^9$

$GHSERNI\,(298.15 < T < 1728) = -5179.159 + 117.854\,T - 22.096\,T\ln T - 0.0048407\,T^2$

$GHSERNI\,(1728 < T < 6000) = -27\,840.655 + 279.135\,T - 43.1\,T\ln T + 1.12754E + 31/T^9$

$GO2GAS\,(298.15 < T < 1000) = -6961.74451 - 51.0057202\,T - 22.2710136\,T\ln T - 0.0101977469\,T^2 + 1.32369208E - 06\,T^3 - 76729.7484/T$

Table 5 (*continued*)

GO2GAS$(1000 < T < 3300) = -13\,137.5203 + 25.3200332\,T - 33.627603\,T\ln T - 0.00119159274\,T^2 + 1.35611111E - 08\,T^3 + 525809.556/T$

GO2GAS$(3300 < T < 6000) = -27\,973.4908 + 62.5195726\,T - 37.9072074\,T\ln T - 8.50483772E - 04\,T^2 + 2.14409777E - 08\,T^3 + 8766\,421.4/T$

Halite: $(Cr^{3+}, Fe^{2+}, Fe^{3+}, Ni^{2+}, Ni^{3+}, Va)_1(O^{2-})_1$

$^oG_{Cr+3:O-2} - H^{SER}_{Cr} - H^{SER}_O = $ CWUSTITE

$^oG_{Fe+2:O-2} - H^{SER}_{Fe} - H^{SER}_O = $ GWUSTITE

$^oG_{Fe+3:O-2} - H^{SER}_{Fe} - H^{SER}_O = 1.25$AWUSTITE $+ 1.25$GWUSTITE

$^oG_{Ni+2:O-2} - H^{SER}_{Ni} - H^{SER}_O = $ GNIO

$^oG_{Ni+3:O-2} - H^{SER}_{Ni} - H^{SER}_O = $ GNIO $+ 132\,919.5 - 64.8855\,T$

$^oG_{Va:O-2} - H^{SER}_O = 0$

$^0L_{Cr+3,Fe+2:O-2} = 12\,500$

$^0L_{Cr+3,Ni+2:O-2} = 61\,000 - 26\,T$[a]

$^0L_{Fe+2,Fe+3:O-2} = -12\,324.4$

$^1L_{Fe+2,Fe+3:O-2} = 20\,070$

$^0L_{Fe+2,Ni+2:O-2} = -21\,995.7281 + 19.7411922\,T$

$^1L_{Fe+2,Ni+2:O-2} = -3335.37286$

$^0L_{Fe+3,Ni+2:O-2} = 64\,792.4377$

For compounds without Fe ions: $^oT_C = 519$

$^o\beta = 0.9873$

AWUSTITE $= -55384 + 27.888\,T$

CWUSTITE$(298.15 < T < 1000) = -563\,748.9 + 407.4569\,T - 66.02315\,T\ln T + 0.002628\,T^2 - 6.944225E - 07\,T^3 + 750881/T$

CWUSTITE$(1000 < T < 6000) = -558\,473.9 + 350.7812\,T - 57.76905\,T\ln T - 0.00310246\,T^2 + 5.034917E - 08\,T^3 + 119\,974.7/T$

GWUSTITE $= -279\,318 + 252.848\,T - 46.12826\,T\ln T - 0.0057402984\,T^2$

GNIO$(298.15 < T < 1000) = -254\,927.2 + 276.208\,T - 46.0391\,T\ln T - 0.00931454\,T^2 + 1.29092E - 06\,T^3 + 382\,916/T$

GNIO$(1000 < T < 1800) = -256\,835.2 + 340.043\,T - 56.36068\,T\ln T + 0.00254106\,T^2 - 8.11809E - 07\,T^3 + 1270/T$

GNIO$(1800 < T < 6000) = -259\,131.4 + 337.305\,T - 55.75758\,T\ln T + 0.00220246\,T^2 - 7.80093E - 07\,T^3$

Corundum: $(Cr^{+2}, Cr^{+3}, Fe^{+2}, Fe^{+3})_2(Cr^{+3}, Fe^{+3}, Ni^{+2}, Va)_1(O^{-2})_3$

$^oG_{Cr+2:Cr+3:O-2} - 3H^{SER}_{Cr} - 3H^{SER}_O = $ GCR2O3 $+ 665\,910$

$^oG_{Cr+3:Cr+3:O-2} - 3H^{SER}_{Cr} - 3H^{SER}_O = $ GCR2O3 $- 232\,227.2 + 241.3793\,T$

$^oG_{Cr+2:Fe+3:O-2} - 2H^{SER}_{Cr} - H^{SER}_{Fe} - 3H^{SER}_O = $ GCR2O3 $+ 300\,000$[a]

$^oG_{Cr+3:Fe+3:O-2} - 2H^{SER}_{Cr} - H^{SER}_{Fe} - 3H^{SER}_O = $ GCR2O3 $+ 300\,000$[a]

$^oG_{Cr+2:Ni+2:O-2} - 2H^{SER}_{Cr} - H^{SER}_{Ni} - 3H^{SER}_O = $ GCR2O3 $+ 665\,910$

$^oG_{Cr+3:Ni+2:O-2} - 2H^{SER}_{Cr} - H^{SER}_{Ni} - 3H^{SER}_O = $ GCR2O3 $+ 28048.1 + 54.4\,T$

$^oG_{Cr+2:Va:O-2} - 2H^{SER}_{Cr} - 3H^{SER}_O = $ GCR2O3

$^oG_{Cr+3:Va:O-2} - 2H^{SER}_{Cr} - 3H^{SER}_O = $ GCR2O3

$^oG_{Fe+2:Cr+3:O-2} - H^{SER}_{Cr} - 2H^{SER}_{Fe} - 3H^{SER}_O = $ GFE2O3 $+ 300\,000$[a]

$^oG_{Fe+3:Cr+3:O-2} - H^{SER}_{Cr} - 2H^{SER}_{Fe} - 3H^{SER}_O = $ GFE2O3 $+ 300\,000$

$^oG_{Fe+2:Fe+3:O-2} - 3H^{SER}_{Fe} - 3H^{SER}_O = $ GFE2O3 $+ 85\,000$

$^oG_{Fe+3:Fe+3:O-2} - 3H^{SER}_{Fe} - 3H^{SER}_O = $ GFE2O3 $+ 85\,000$

$^oG_{Fe+2:Ni+2:O-2} - 2H^{SER}_{Fe} - H^{SER}_{Ni} - 3H^{SER}_O = $ GFE2O3 $+ 300\,000$[a]

$^oG_{Fe+3:Ni+2:O-2} - 2H^{SER}_{Fe} - H^{SER}_{Ni} - 3H^{SER}_O = $ GFE2O3 $+ 300\,000$

$^oG_{Fe+2:Va:O-2} - 2H^{SER}_{Fe} - 3H^{SER}_O = $ GFE2O3

$^oG_{Fe+3:Va:O-2} - 2H^{SER}_{Fe} - 3H^{SER}_O = $ GFE2O3

$^0L_{Cr+3,Fe+3:Va:O-2} = -16\,250 + 12.5\,T$

$^0T_{CCr+2:*:O-2} = {}^oT_{CCr+3:*:O-2} = -918$

$^0T_{CFe+3:*:O-2} = {}^oT_{CFe+2:*:O-2} = -2867$

$^0\beta_{Cr+2:*:O-2} = {}^o\beta_{Cr+3:*:O-2} = -5.814$

$^0\beta_{Fe+2:*:O-2} = {}^o\beta_{Fe+3:*:O-2} = -25.1$

GCR2O3$(298.15 < T < 1000) = -1\,177\,497.8 + 814.9138\,T - 132.046\,T\ln T + 0.005256015\,T^2 - 1.38885E - 06\,T^3 + 1501761/T$

GCR2O3$(1000 < T < 6000) = -1\,166\,947.9 + 701.5624\,T - 115.5381\,T\ln T - 0.00620492\,T^2 + 1.00698E - 07\,T^3 + 239949/T$

GFE2O3 $= -858\,683 + 827.946\,T - 137.0089\,T\ln T + 1453\,810/T$

Spinel: $(Cr^{+2}, Cr^{+3}, Fe^{+2}, Fe^{+3}, Ni^{+2})_1(Cr^{+3}, Fe^{+2}, Fe^{+3}, Ni^{+2}, Va)_2(Cr^{+2}, Fe^{+2}, Va)_2(O^{-2})_4$

$^oG_{Cr+2:Cr+3:Fe+2:O-2} - 3H^{SER}_{Cr} - 2H^{SER}_{Fe} - 4H^{SER}_O = 10.5F - 1.5G - 1.5B + D + R + S$

$^oG_{Cr+3:Cr+3:Fe+2:O-2} - 3H^{SER}_{Cr} - 2H^{SER}_{Fe} - 4H^{SER}_O = 10.5F - 1.5G - 1.5B + D + R$

$^oG_{Fe+2:Cr+3:Fe+2:O-2} - 2H^{SER}_{Cr} - 3H^{SER}_{Fe} - 4H^{SER}_O = 7F + 2G - B + D$

$^oG_{Fe+3:Cr+3:Fe+2:O-2} - 2H^{SER}_{Cr} - 3H^{SER}_{Fe} - 4H^{SER}_O = 7F + 2G - 2B + D$

$^oG_{Ni+2:Cr+3:Fe+2:O-2} - 2H^{SER}_{Cr} - H^{SER}_{Ni} - 2H^{SER}_{Fe} - 4H^{SER}_O = H + 2G - B + D$

$^oG_{Cr+2:Fe+2:Fe+2:O-2} - H^{SER}_{Cr} - 4H^{SER}_{Fe} - 4H^{SER}_O = 3.5F + 5.5G - 0.5B + D + R + S$

$^oG_{Cr+3:Fe+2:Fe+2:O-2} - H^{SER}_{Cr} - 4H^{SER}_{Fe} - 4H^{SER}_O = 3.5F + 5.5G - 0.5B + D + R$

(*continued on next page*)

Table 5 (*continued*)

$${}^oG_{Fe^{+2}:Fe^{+2}:Fe^{+2}:O^{-2}} -5H_{Fe}^{SER} - 4H_O^{SER} = 9G + D$$

$${}^oG_{Fe^{+3}:Fe^{+2}:Fe^{+2}:O^{-2}} -5H_{Fe}^{SER} - 4H_O^{SER} = 9G - B + D$$

$${}^oG_{Ni^{+2}:Fe^{+2}:Fe^{+2}:O^{-2}} -H_{Ni}^{SER} - 4H_{Fe}^{SER} - 4H_O^{SER} = 7E + 2G + D$$

$${}^oG_{Cr^{+2}:Fe^{+3}:Fe^{+2}:O^{-2}} -H_{Cr}^{SER} - 4H_{Fe}^{SER} - 4H_O^{SER} = 3.5F + 5.5G - 1.5B + D + R + S$$

$${}^oG_{Cr^{+3}:Fe^{+3}:Fe^{+2}:O^{-2}} -H_{Cr}^{SER} - 4H_{Fe}^{SER} - 4H_O^{SER} = 3.5F + 5.5G - 1.5B + D + R$$

$${}^oG_{Fe^{+2}:Fe^{+3}:Fe^{+2}:O^{-2}} -5H_{Fe}^{SER} - 4H_O^{SER} = 9G - B + D$$

$${}^oG_{Fe^{+3}:Fe^{+3}:Fe^{+2}:O^{-2}} -5H_{Fe}^{SER} - 4H_O^{SER} = 9G - 2B + D$$

$${}^oG_{Ni^{+2}:Fe^{+3}:Fe^{+2}:O^{-2}} -H_{Ni}^{SER} - 4H_{Fe}^{SER} - 4H_O^{SER} = 7E + 2G - B + D$$

$${}^oG_{Cr^{+2}:Ni^{+2}:Fe^{+2}:O^{-2}} -H_{Cr}^{SER} - 2H_{Ni}^{SER} - 2H_{Fe}^{SER} - 4H_O^{SER} = 14E - A + 3.5F - 8.5G + 0.5B + D + R + S$$

$${}^oG_{Cr^{+3}:Ni^{+2}:Fe^{+2}:O^{-2}} -H_{Cr}^{SER} - 2H_{Ni}^{SER} - 2H_{Fe}^{SER} - 4H_O^{SER} = H + 71546 + 2G - B + D$$

$${}^oG_{Fe^{+2}:Ni^{+2}:Fe^{+2}:O^{-2}} -2H_{Ni}^{SER} - 3H_{Fe}^{SER} - 4H_O^{SER} = 14E - A - 5G + B + D$$

$${}^oG_{Fe^{+3}:Ni^{+2}:Fe^{+2}:O^{-2}} -2H_{Ni}^{SER} - 3H_{Fe}^{SER} - 4H_O^{SER} = 14E - A - 5G + D$$

$${}^oG_{Ni^{+2}:Ni^{+2}:Fe^{+2}:O^{-2}} -3H_{Ni}^{SER} - 2H_{Fe}^{SER} - 4H_O^{SER} = 21E - A - 12G + B + D$$

$${}^oG_{Cr^{+2}:Va:Fe^{+2}:O^{-2}} -H_{Cr}^{SER} - 2H_{Fe}^{SER} - 4H_O^{SER} = 3.5F + 3.5G - 1.5B + C + D + R + S$$

$${}^oG_{Cr^{+3}:Va:Fe^{+2}:O^{-2}} -H_{Cr}^{SER} - 2H_{Fe}^{SER} - 4H_O^{SER} = 3.5F + 3.5G - 1.5B + C + D + R$$

$${}^oG_{Fe^{+2}:Va:Fe^{+2}:O^{-2}} -3H_{Fe}^{SER} - 4H_O^{SER} = 7G - B + C + D$$

$${}^oG_{Fe^{+3}:Va:Fe^{+2}:O^{-2}} -3H_{Fe}^{SER} - 4H_O^{SER} = 7G - 2B + C + D$$

$${}^oG_{Ni^{+2}:Va:Fe^{+2}:O^{-2}} -H_{Ni}^{SER} - 2H_{Fe}^{SER} - 4H_O^{SER} = 7E - B + C + D$$

$${}^oG_{*:*:Cr^{+2}:O^{-2}} = {}^oG_{*:*:Fe^{+2}:O^{-2}}$$

$${}^oG_{Cr^{+2}:Cr^{+3}:Va:O^{-2}} -3H_{Cr}^{SER} - 4H_O^{SER} = 10.5F - 3.5G - 0.5B + R + S$$

$${}^oG_{Cr^{+3}:Cr^{+3}:Va:O^{-2}} -3H_{Cr}^{SER} - 4H_O^{SER} = 10.5F - 3.5G - 0.5B + R$$

$${}^oG_{Fe^{+2}:Cr^{+3}:Va:O^{-2}} -2H_{Cr}^{SER} - H_{Fe}^{SER} - 4H_O^{SER} = 7F$$

$${}^oG_{Fe^{+3}:Cr^{+3}:Va:O^{-2}} -2H_{Cr}^{SER} - H_{Fe}^{SER} - 4H_O^{SER} = 7F - B$$

$${}^oG_{Ni^{+2}:Cr^{+3}:Va:O^{-2}} -2H_{Cr}^{SER} - H_{Ni}^{SER} - 4H_O^{SER} = H$$

$${}^oG_{Cr^{+2}:Fe^{+2}:Va:O^{-2}} -H_{Cr}^{SER} - 2H_{Fe}^{SER} - 4H_O^{SER} = 3.5F + 3.5G + 0.5B + R + S$$

$${}^oG_{Cr^{+3}:Fe^{+2}:Va:O^{-2}} -H_{Cr}^{SER} - 2H_{Fe}^{SER} - 4H_O^{SER} = 3.5F + 3.5G + 0.5B + R$$

$${}^oG_{Fe^{+2}:Fe^{+2}:Va:O^{-2}} -3H_{Fe}^{SER} - 4H_O^{SER} = 7G + B$$

$${}^oG_{Fe^{+3}:Fe^{+2}:Va:O^{-2}} -3H_{Fe}^{SER} - 4H_O^{SER} = 7G$$

$${}^oG_{Ni^{+2}:Fe^{+2}:Va:O^{-2}} -2H_{Fe}^{SER} - H_{Ni}^{SER} - 4H_O^{SER} = 7E + B$$

$${}^oG_{Cr^{+2}:Fe^{+3}:Va:O^{-2}} -H_{Cr}^{SER} - 2H_{Fe}^{SER} - 4H_O^{SER} = 3.5F + 3.5G - 0.5B + R + S$$

$${}^oG_{Cr^{+3}:Fe^{+3}:Va:O^{-2}} -H_{Cr}^{SER} - 2H_{Fe}^{SER} - 4H_O^{SER} = 3.5F + 3.5G - 0.5B + R$$

$${}^oG_{Fe^{+2}:Fe^{+3}:Va:O^{-2}} -3H_{Fe}^{SER} - 4H_O^{SER} = 7G$$

$${}^oG_{Fe^{+3}:Fe^{+3}:Va:O^{-2}} -3H_{Fe}^{SER} - 4H_O^{SER} = 7G - B$$

$${}^oG_{Ni^{+2}:Fe^{+3}:Va:O^{-2}} -2H_{Fe}^{SER} - H_{Ni}^{SER} - 4H_O^{SER} = 7E$$

$${}^oG_{Cr^{+2}:Ni^{+2}:Va:O^{-2}} -H_{Cr}^{SER} - 2H_{Ni}^{SER} - 4H_O^{SER} = 14E - A + 3.5F - 10.5G + 1.5B + R + S$$

$${}^oG_{Cr^{+3}:Ni^{+2}:Va:O^{-2}} -H_{Cr}^{SER} - 2H_{Ni}^{SER} - 4H_O^{SER} = 2H + 143092 - 10.5F + 3.5G + 0.5B - R$$

$${}^oG_{Fe^{+2}:Ni^{+2}:Va:O^{-2}} -H_{Fe}^{SER} - 2H_{Ni}^{SER} - 4H_O^{SER} = 14E - A - 7G + 2B$$

$${}^oG_{Fe^{+3}:Ni^{+2}:Va:O^{-2}} -H_{Fe}^{SER} - 2H_{Ni}^{SER} - 4H_O^{SER} = 14E - A - 7G + B$$

$${}^oG_{Ni^{+2}:Ni^{+2}:Va:O^{-2}} 3H_{Ni}^{SER} - 4H_O^{SER} = 21E - A - 14G + 2B$$

$${}^oG_{Cr^{+2}:Va:Va:O^{-2}} -H_{Cr}^{SER} - 4H_O^{SER} = 3.5F + 1.5G - 0.5B + C + R + S$$

$${}^oG_{Cr^{+3}:Va:Va:O^{-2}} -H_{Cr}^{SER} - 4H_O^{SER} = 3.5F + 1.5G - 0.5B + C + R$$

$${}^oG_{Fe^{+2}:Va:Va:O^{-2}} -H_{Fe}^{SER} - 4H_O^{SER} = 5G + C$$

$${}^oG_{Fe^{+3}:Va:Va:O^{-2}} -H_{Fe}^{SER} - 4H_O^{SER} = 5G - B + C$$

$${}^oG_{Ni^{+2}:Va:Va:O^{-2}} -H_{Ni}^{SER} - 4H_O^{SER} = 7E - 2G + C$$

$${}^0L_{Cr^{+3},Fe^{+2}:Cr^{+3}:Va:O^{-2}} = 20\,000$$

$${}^0L_{Cr^{+3},Fe^{+2}:Fe^{+3}:Va:O^{-2}} = 20\,000$$

$${}^0L_{Cr^{+3},Fe^{+2}:Fe^{+2}:Va:O^{-2}} = 20\,000$$

$${}^0L_{Cr^{+3},Fe^{+2}:Va:Va:O^{-2}} = 20\,000$$

$${}^0L_{Cr^{+3},Ni^{+2}:Ni^{+2}:Va:O^{-2}} = DELTAG$$

$${}^0L_{Cr^{+3},Ni^{+2}:Cr^{+3}:Va:O^{-2}} = DELTAG$$

$${}^0L_{Fe^{+2}:Cr^{+3},Fe^{+2}:Va:O^{-2}} = 152380 - 60\,T$$

$${}^0L_{Fe^{+2}:Cr^{+3},Fe^{+3}:Va:O^{-2}} = -24\,942 + 28.5714\,T$$

$${}^0L_{Fe^{+2}:Cr^{+3},Va:Va:O^{-2}} = 5000$$

$${}^1L_{Fe^{+2}:Cr^{+3},Va:Va:O^{-2}} = 150\,000$$

$${}^0L_{Fe^{+3}:Cr^{+3},Fe^{+2}:Va:O^{-2}} = 152\,380 - 60\,T$$

$${}^0L_{Fe^{+3}:Cr^{+3},Va:Va:O^{-2}} = 5000$$

Table 5 (*continued*)

$^1L_{Fe^{+3}:Cr^{+3},Va:Va:O^{-2}} = 150\,000$

$^0L_{Fe^{+3}:Cr^{+3},Ni^{+2}:Va:O^{-2}} = 122\,000 - 79\,T$[a]

$^0L_{Fe^{+3},Ni^{+2}:Cr^{+3}:Va:O^{-2}} = -16\,000$[a]

Magnetic properties:

For compounds containing only Fe cations $T_C = 848$ and $\beta = 44.54$

For compounds containing only Cr or Cr+Fe cations $T_C = 100$ and $\beta = 0.9$

For compounds containing only Ni or Fe+Ni cations $T_C = 858$[a] and $\beta = 0$[a]

All other compounds $T_C = 0$ and $\beta = 0$

$^0\beta_{Fe^{+3}:Fe^{+3},Ni^{+2}:Va:O^{-2}} = -69.61$[a]

$A = 142\,000$[a]

$B = 46\,826 - 27.266\,T$

$C = 120\,730 - 20.102\,T$

$D = 402\,520 - 30.529\,T$

$E = -153\,200 + 173.55\,T - 28.259\,T\ln T - 3.2E-04\,T^2 + 291\,000/T$[a]

$F = -214\,607.7 + 138.83\,T - 23.28714\,T\ln T - 0.001595929\,T^2 + 227729.3/T$

$G = -161731 + 144.873\,T - 24.9879\,T\ln T - 0.0011952256\,T^2 + 206\,520/T$

$H = -1442\,728.78 + 1005.1\,T - 167.1508\,T\ln T - 0.00893284\,T^2 + 1052\,276/T$

$R = 156\,000 - 3.37\,T$

$S = 46\ 28.95 + 38.73173\,T - 11.58574\,T\ln T + 0.006411774\,T^2$

$DELTAG = 1.5H - 10.5E + 0.5A + 10.5G - 0.5B - 10.5F - R + 71546$

Fcc: $(Cr, Fe, Ni)_1 (O, Va)_1$

$^oG_{Cr:O} - H_{Cr}^{SER} - H_O^{SER} = GCRFCC + 0.5GO2GAS + 65\,T$

$^oG_{Fe:O} - H_{Fe}^{SER} - H_O^{SER} = GFEFCC + 0.5GO2GAS + 65\,T$

$^oG_{Ni:O} - H_{Ni}^{SER} - H_O^{SER} = GHSERNI + 0.5GO2GAS + 65\,T$

$^oG_{Cr:Va} - H_{Cr}^{SER} = GCRFCC$

$^oG_{Fe:Va} - H_{Fe}^{SER} = GFEFCC$

$^oG_{Ni:Va} - H_{Ni}^{SER} = GHSERNI$

$^0L_{Cr:O,Va} = -170\,000 + 20\,T$

$^0L_{Fe:O,Va} = -168\,758 + 19.17\,T$

$^0L_{Ni:O,Va} = -165\,608 + 32.24\,T$

$^0L_{Cr,Fe:Va} = 10\,833 - 7.477\,T$

$^1L_{Cr,Fe:Va} = 1410$

$^0L_{Cr,Ni:Va} = 8030 - 12.8801\,T$

$^1L_{Cr,Ni:Va} = 33\,080 - 16.0362\,T$

$^0L_{Fe,Ni:Va} = -12\,054.355 + 3.27413\,T$

$^1L_{Fe,Ni:Va} = 11\,082.13 - 4.45077\,T$

$^2L_{Fe,Ni:Va} = -725.805174$

$^0L_{Cr,Fe,Ni:Va} = 16\,580 - 9.783\,T$

$^0T C_{Cr:Va} = -1109$

$^0T C_{Fe:Va} = -201$

$^0T C_{Ni:Va} = 633$

$^0T C_{Cr,Ni:Va} = -3605$

$^0T C_{Fe,Ni:Va} = 2133$

$^1T C_{Fe,Ni:Va} = -682$

$^0\beta_{Cr:Va} = -2.46$

$^0\beta_{Fe:Va} = -2.1$

$^0\beta_{Ni:Va} = 0.52$

$^0\beta_{Cr,Ni:Va} = -1.91$

$^0\beta_{Fe,Ni:Va} = 9.55$

$^1\beta_{Fe,Ni:Va} = 7.23$

$^2\beta_{Fe,Ni:Va} = 5.93$

$^3\beta_{Fe,Ni:Va} = 6.18$

$GCRFCC = 7284 + 0.163\,T + GHSERCR$

$GFEFCC(298.15 < T < 1811) = -1462.4 + 8.282\,T - 1.15\,T\ln T + 6.4E-04\,T^2 + GHSERFE$

$GFEFCC(1811 < T < 6000) = -1713.815 + .94001\,T + 4.9251E+30/T^9 + GHSERFE$

Bcc: $(Cr, Fe, Ni)_1 (O, Va)_3$

$^oG_{Cr:O} - H_{Cr}^{SER} - 3H_O^{SER} = GHSERCR + 1.5GO2GAS + 195\,T$

$^oG_{Fe:O} - H_{Fe}^{SER} - 3H_O^{SER} = GHSERFE + 1.5GO2GAS + 195\,T$

$^oG_{Ni:O} - H_{Ni}^{SER} - 3H_O^{SER} = GNIBCC + 1.5GO2GAS + 195\,T$

$^oG_{Cr:Va} - H_{Cr}^{SER} = GHSERCR$

$^oG_{Fe:Va} - H_{Fe}^{SER} = GHSERFE$

$^oG_{Ni:Va} - H_{Ni}^{SER} = GHSERNI + 8715.084 - 3.556\,T$

$^0L_{Cr:O,Va} = -673\,435 + 27.86\,T$

$^0L_{Fe:O,Va} = -517\,549 + 71.83\,T$

Table 5 (*continued*)

$$^0L_{\text{Ni:O,Va}} = -400\,000 + 50\,T$$
$$^0L_{\text{Cr,Fe:Va}} = 20\,500 - 9.68\,T$$
$$^0L_{\text{Cr,Ni:Va}} = 17\,170 - 11.8199\,T$$
$$^1L_{\text{Cr,Ni:Va}} = 34\,418 - 11.8577\,T$$
$$^0L_{\text{Fe,Ni:Va}} = -956.63 - 1.28726\,T$$
$$^1L_{\text{Fe,Ni:Va}} = 1789.03 - 1.92912\,T$$
$$^0L_{\text{Cr,Fe,Ni:Va}} = -2673 + 2.0415\,T$$
$$^0TC_{\text{Cr:Va}} = -311.5$$
$$^0TC_{\text{Fe:Va}} = +1043$$
$$^0TC_{\text{Ni:Va}} = +575$$
$$^0TC_{\text{Cr,Fe:Va}} = 1650$$
$$^1TC_{\text{Cr,Fe:Va}} = 550$$
$$^0TC_{\text{Cr,Ni:Va}} = 2373$$
$$^1TC_{\text{Cr,Ni:Va}} = 617$$
$$^0\beta_{\text{Cr:Va}} = -0.008$$
$$^0\beta_{\text{Fe:Va}} = 2.22$$
$$^0\beta_{\text{Ni:Va}} = +0.85$$
$$^0\beta_{\text{Cr,Fe:Va}} = -0.85$$
$$^0\beta_{\text{Cr,Ni:Va}} = 4$$
$$\text{GNIBCC} = 8715.084 - 3.556\,T + \text{GHSERNI}$$

Gas: (Cr, CrO, CrO_2, CrO_3, Cr_2, Cr_2O, Cr_2O_2, Cr_2O_3, Fe, FeO, FeO_2, Fe_2, Ni, NiO, Ni_2, O, O_2, O_3)

From SGTE substance database [22]

 a Parameters assessed in this work.

References

[1] R. Luoma, Doctoral thesis, Acta Polytechnica Scandinavia, Chemical Technology Series No. 292, 2002.
[2] F. Sommer, Z. Metallkd. 73 (1982) 72–76.
[3] J. Taylor, A. Dinsdale, Z. Metallkde. 81 (1990) 354–366.
[4] J. Taylor, A. Dinsdale, Z. Metallkde. 84 (1993) 335–345.
[5] R. Luoma, Calphad 19 (1995) 279–295.
[6] B.-J. Lee, Unpublished revision of C–Cr–Fe–Ni.
[7] B.-J. Lee, Calphad 17 (1993) 251–268.
[8] M. Hillert, B. Jansson, B. Sundman, J. Gren, Metall. Trans. 16A (1985) 261–266.
[9] B. Sundman, Calphad 15 (1991) 109–119.
[10] M. Hillert, J. Alloys Compd. 320 (2001) 161–176.
[11] H. Mao, M. Hillert, M. Selleby, B. Sundman, J. Am. Ceram. Soc. 89 (2006) 298–308.
[12] H. Mao, O. Fabrichnaya, M. Selleby, B. Sundman, J. Mater. Res. 20 (2005) 975–986.
[13] N. Saunders, A. Miodownik, Calphad (Calculation of Phase Diagrams): A Comprehensive Guide, Pergamon Press, 1998.
[14] H. Lukas, S. Fries, B. Sundman, Computational Thermodynamics, The Calphad Method, Cambridge, 2007.
[15] G. Inden, Z. Met. kd. 66 (1975) 577.
[16] M. Hillert, M. Jarl, Calphad 2 (1978) 227–238.
[17] B. Sundman, J. Phase Equilibria 12 (1991) 127–140.
[18] M. Selleby, B. Sundman, Calphad 20 (1996) 381–392.
[19] H. Mao, M. Selleby, B. Sundman, Calphad 28 (2004) 307–312.
[20] J. Topfer, S. Aggarwal, R. Dieckmann, Solid State Ion. 81 (1995) 251–266.
[21] B. Hallstedt, Calphad 16 (1992) 53–61.
[22] SSUB3: SGTE substance database, Provided by Thermo-Calc Software v3.2 2002/2004.
[23] A. Dinsdale, Calphad 15 (1991) 317–425.
[24] J.-O. Andersson, B. Sundman, Calphad 11 (1987) 83–92.
[25] A. Dinsdale, T. Chart, MTDS NPL, Unpublished work; CR-NI.
[26] M. Kowalski, P. Spencer, Calphad 19 (1995) 229–243.
[27] A. Dinsdale, T. Chart, MTDS NPL, Unpublished work; FE-NI.
[28] E. Povoden, N. Grundy, L. Gauckler, J. Phase Equilib. Diffus. 27 (2006) 353–362.
[29] N. Toker, L. Darken, M.A. , Metall. Trans. B 22 (2) (1991) 225–232.
[30] Y. Ol'shanskii, V. Shlepov, Dokl. Akad. Nauk SSSR 91 (1953) 561–564.
[31] J. Greig, E. Posnjak, H. Merwin, R. Sosman, Am. J. Sci. 30 (1935) 239–316.
[32] M. Heinz, K. Koch, D. Janke, Steel Res. 60 (1989) 246–254.
[33] A. Muan, S. Somiya, J. Am. Ceram. Soc. 43 (1960) 204–209.
[34] H.-M. Chen, J. Chipman, Trans. ASM 38 (1947) 70–113.
[35] D. Hilty, W. Forgeng, R. Folkman, J. Metals 7 (1955) 253–268.
[36] H. Sakao, K. Sano, J. Japan Inst. Met. 26 (1962) 236–240.
[37] N. Iwamoto, M. Takano, H. Kanayama, A. Adachi, Tetsu To Hagane 56 (1970) 727–733.
[38] C. Kim, A. McLean, Metall. Trans. B 10B (1979) 585–594.
[39] B. Belov, I. Novokhatskii, Zh. Fiz. Khim 48 (1974) 2860–2864.
[40] B. Belov, I. Novokhatskii, L. Rusakov, A. Gorokh, A. Savinskaya, Zh. Fiz. Khim 42 (1968) 1635–1637.
[41] R. Fruehan, Trans. Met. Soc. AIME 245 (1969) 1215–1218.
[42] V. Averin, P. Cherkasov, A. Samarin, Issled po Zharaprochn, Splavam. Akad. Nauk. SSSR 9 (1962) 204–218.
[43] B. Belov, I. Novokhatskii, Russ. Met. 5 (1970) 52–55.
[44] H. Sakao, K. Sano, J. Japan Inst. Met. 26 (1962) 240–244.
[45] C. Greskovich, J. Am. Ceram. Soc. 53 (1970) 498–502.
[46] C.-H. Chen, M. Notis, D. Williams, J. Am. Ceram. Soc. 66 (1983) 566–571.
[47] G. Meier, R. Rapp, Z. Phys. Chem. 74 (1971) 168–189.
[48] H. Davies, W. Smeltzer, J. Electrochem. Soc. 121 (1974) 543–549.
[49] J. Robertson, A. Pointon, Solid State Commun. 4 (1966) 257–259.
[50] I. Barin, O. Knacke, O. Kubaschewski, Thermodynamic Properties of Inorganic Substances, Springer-Verlag, New York, 1973, Supplement 1977.
[51] G. Chachanidze, Izvest. Akad. Nauk. SSSR, Neorg. Mater. 26 (1970) 376–379.
[52] F. Schneider, H. Schmalzried, Z. Phys. Chem. Neue Folge 166 (1990) 1–18.
[53] A. Paladino, J. Am. Ceram. Soc. 42 (1959) 168–175.
[54] H. Schmalzried, J. Tretjakov, Ber. Bunsenges Phys. Chem. 70 (1966) 180–189.
[55] A. Zalazinskii, V. Balakirev, G. Chufarov, Russ. J. Phys. Chem. 47 (1973) 259–261.
[56] A. Dalvi, R. Sridhar, Can. Metall. Q. 15 (1976) 349–357.
[57] H. Davies, W. Smeltzer, J. Electrochem. Soc. 119 (1972) 1362–1368.
[58] M.-C. Trinel-Dufour, G. Pouillard, P. Perrot, J. Chem. Res. (M) (1979) 2401–2423.
[59] Y. Kuznetsov, Nauch. Tr. Mosk. In-t., Stali i Splavov (1983) 68–77.
[60] B. Gries, Diplomarbeit, Universität Hannover.
[61] V. Shevtsov, Izvest. Akad. Nauk. SSSR, Metally 2 (1979) 71–74.
[62] S. Ziemniak, A. Gaddipati, P. Sander, J. Phys. Chem. Solids 66 (2005) 1112–1121.
[63] J.O. Andersson, T. Helander, L. Höglund, P.F. Shi, B. Sundman, Calphad 26 (2002) 273–312.